Biomacromolecules

Article

Impact of polymer-TLR-7/8 agonist (adjuvant) morphology on the potency and mechanism of CD8 T cell induction

Geoffrey M. Lynn, Petr Chytil, Joseph R. Francica, Anna Lagova, Gray Kueberuwa, Andrew S. Ishizuka, Neeha Zaidi, Ramiro A. Ramirez-Valdez, Nicolas J. Blobel, Faezzah Baharom, Joseph Leal, Amy Q. Wang, Michael Y. Gerner, Tomáš Etrych, Karel Ulbrich, Leonard W. Seymour, Robert A. Seder, and Richard Laga

Biomacromolecules, **Just Accepted Manuscript** • DOI: 10.1021/acs.biomac.8b01473 • Publication Date (Web): 04 Jan 2019

Impact of polymer-TLR-7/8 agonist (adjuvant) morphology on the potency and mechanism of CD8 T cell induction

Geoffrey M. Lynn[a], Petr Chytil[b], Joseph R. Francica[a], Anna Lagová[c], Gray Kueberuwa[c], Andrew S. Ishizuka[a], Neeha Zaidi[a], Ramiro A. Ramirez-Valdez[a], Nicolas J. Blobel[a], Faezzah Baharom[a], Joseph Leal[d], Amy Q. Wang[e], Michael Y. Gerner[d], Tomáš Etrych[b], Karel Ulbrich[b], Leonard W. Seymour[c], Robert A. Seder[a, ‡] and Richard Laga[b,c, ‡,]*

[a]Vaccine Research Center, National Institute of Allergy and Infectious diseases, National Institutes of Health, 40 Convent Drive, Bethesda, MD 20892, USA

[b]Institute of Macromolecular Chemistry, Czech Academy of Sciences, Heyrovského nám. 2, 162 06 Prague 6, Czech Republic

[c]Department of Oncology, University of Oxford, Old Road Campus Research Building, Oxford, OX3 7DQ, United Kingdom

[d]Department of Immunology, University of Washington, South Lake Union E-411, 750 Republican St., Seattle, WA 98109

[e]Therapeutics for Rare and Neglected Diseases, National Center for Advancing Translational Sciences, 9800 Medical Center Drive, Rockville, MD 20850.

KEYWORDS

Adjuvants, hydrophilic polymers, Toll-like receptor-7 & -8 agonists, polymer immunostimulants, cellular immunity, vaccine delivery

ABSTRACT

Small molecule Toll-like receptor-7 and -8 agonists (TLR-7/8a) can be used as vaccine adjuvants to induce CD8 T cell immunity but require formulations that prevent systemic toxicity and focus adjuvant activity in lymphoid tissues. Here, we covalently attached TLR-7/8a to polymers of varying composition, chain architecture and hydrodynamic behavior (~ 300 nm submicron particles, ~ 10 nm micelles and ~ 4 nm flexible random coils) and evaluated how these parameters of polymer-TLR-7/8a conjugates impact

adjuvant activity in vivo. Attachment of TLR-7/8a to any of the polymer compositions resulted in a nearly 10-fold reduction in systemic cytokines (toxicity). Moreover, both lymph node cytokine production and the magnitude of CD8 T cells induced against protein antigen increased with increasing polymer-TLR-7/8a hydrodynamic radius, with the submicron particle inducing the highest magnitude responses. Notably, CD8 T cell responses induced by polymer-TLR-7/8a were dependent on CCR2+ monocytes and IL-12, whereas responses by a small molecule TLR-7/8a that unexpectedly persisted in vaccine-site draining lymph nodes (T1/2 = 15 hours) had less dependence on monocytes and IL-12 but required Type I IFNs. This study shows how modular properties of synthetic adjuvants can be chemically programmed to alter immunity in vivo through distinct immunological mechanisms.

INTRODUCTION

While most currently licensed vaccines mediate protection through antibodies [1], vaccines that generate CD8 T cell immunity are needed for certain infectious diseases (*e.g.*, Malaria [2]and Ebola [3]) as well as cancer [4-6]. A promising vaccine approach to elicit CD8 T cell immunity is to combine protein or peptide antigens with specific adjuvants that activate antigen-presenting cells (APCs) that promote the priming and expansion of CD8 T cells [7].

Some of the most studied adjuvants for inducing CD8 T cell immunity include a structurally diverse class of synthetic and naturally occurring molecules that bind to specific Toll-like receptors (TLRs) [8]. TLR agonists (TLRa) function as adjuvants by binding to cognate surface *(e.g.*, TLR-1, 2, 4, 5 and 6) or intracellular (*e.g.*, TLR-3, 7, 8 and 9) receptors on antigen-presenting cells (APCs), such as dendritic cells, leading to a downstream signaling cascade that results in APCs migrating from the periphery to draining lymph nodes (DLN); upregulating antigen presentation and co-stimulatory molecule expression; and, producing specific cytokines required for driving T cell responses to co-administered antigen [8].

Particular TLRa can be selected for use in vaccines to induce qualitatively distinct immune responses. Agonists that bind to endosomally localized TLR-7 and -8 (TLR-7/8), which naturally recognize single stranded RNA from viruses [9], have garnered interest for use as vaccine adjuvants based on their ability to induce APCs to produce specific cytokines (*i.e.* IL-12 and Type I Interferons (IFNs)) that promote CD8 T cell immunity [10, 11]. While a broad range of synthetic TLR-7/8a structurally related to the nucleotide bases adenine and guanine have been described [12-15], the imidazoquinoline class, which includes two compounds, Imiquimod (Aldara) and Resiquimod (R848), that are approved by the FDA for the treatment of skin pathologies [14, 16], are some of the most studied and promising for use as adjuvants for inducing CD8 T cell immunity [10]. Despite having favorable immunological characteristics for use as adjuvants for inducing CD8 T cell immunity, imidazoquinoline-based TLR-7/8a are currently restricted to topical uses clinically because these low-molecular-weight, amphiphilic compounds have suboptimal pharmacokinetic (PK) properties for use in parenterally administered vaccines. For instance, following common routes of vaccination (*e.g.*, intramuscular or

subcutaneous), unformulated, small molecule TLR-7/8a rapidly enter the blood and cause systemic immune activation that results in flu-like symptoms in patients [17-20], with only a limited quantity of the agonist reaching lymph nodes where it is needed for priming T cells [21-23]. Furthermore, free TLR-7/8a may have lower avidity for binding cognate receptors or result in suboptimal receptor clustering as compared with natural agonists, which are presented as repeating macromolecular units on pathogen particles [24].

A variety of approaches have been developed to improve the pharmacokinetic properties of TLR-7/8a, and other adjuvants, for use as adjuvants in vaccines. One strategy is to physically entrap the TLR-7/8a within nano- and micro-sized particles based on PLGA [25-27], liposomes [28, 29], polypropylene sulfide-based polymersomes [30], polymer micelles [31] or cross-linked polysaccharides [32]. As an alternative to physically entrapping the adjuvant within particles, which can be limited by relatively low and variable adjuvant loading, TLR-7/8a can be covalently linked ("conjugated") to macromolecular carriers, including proteins[33-35], dendrimers [36] and functionalized

hydrophilic or amphiphilic polymers [37]. Potential advantages of conjugating adjuvants (and/or antigens) to macromolecular carriers is that loading can be controlled by the number of functional groups used for adjuvant attachment and that the macromolecular conjugate is a chemically defined, single molecule that permits facile sterile-filtration but can be chemically programmed for assuming different hydrodynamic properties depending on the environment [21, 38-40].

Prior studies have established that a critical role of adjuvant delivery systems based on particle emulsions and macromolecular conjugates is to physically restrict adjuvant distribution to vaccine-site DLN where T cell priming occurs, while at the same time preventing systemic distribution associated with adjuvant toxicity [21, 41-43]. However, it remains unclear how various characteristics of the delivery platform, such as size and morphology, influence the efficiency and mechanism of the adjuvant for eliciting T cell immunity. Accordingly, while nanoparticles with a size range between ~ 20-200 nm in diameter have been reported to be optimal for promoting T cell immunity based on their ability to passively traffic to lymph nodes and promote uptake by lymph node resident

dendritic cells [24, 44, 45], submicron-sized particles (> 200 nm) that reach lymph nodes through active trafficking by migratory APCs and some passive drainage [46] also induce robust T cell immunity [21, 47]. Moreover, it has not been thoroughly investigated how various properties of macromolecular carriers, including architecture (*e.g.*, di-block versus co-polymer) and hydrodynamic behavior (*e.g.*, random coil, micelle or submicron particle) impact CD8 T cell immunity.

To evaluate how characteristics of the adjuvant carrier impacts CD8 T cell immunity, we synthesized polymer-TLR-7/8a conjugates with different chemical compositions and chain architectures exhibiting distinct hydrodynamic characteristics (random coil, polymer micelle and submicron particle) and evaluated how these parameters impact the efficiency and mechanism of the adjuvant for inducing CD8 T cells *in vivo*. While we previously evaluated how the density of an R848 analog linked to water-soluble and temperature-responsive polymer carriers impacts immunogenicity [21], herein we expanded on this prior work by using a higher potency TLR-7/8a comprising an imidazoquinoline with a C^2-butyl substituent and an N^1-xylylamine substituent, referred

to herein as 2BXy (also known as IMDQ[48]) linked to polymers with different chain architectures and hydrodynamic properties.

The data presented herein provides insights as to how properties of macromolecular conjugates of TLR-7/8a, including polymer chain composition and hydrodynamic behavior, can be chemically tuned to alter the magnitude and quality of innate and adaptive CD8 T cell immunity. Overall, this work has important implications for the development of vaccines for inducing CD8 T cells for the treatment of infectious diseases and cancer.

MATERIALS AND METHODS

Chemicals

(RS)-1-Aminopropan-2-ol, 6-aminohexanoic acid (ε-Ahx), 3-aminopropionic acid (β-Ala), (+)-sodium L-ascorbate, azobisisobutyronitrile (AIBN), 4,4′-azobis(4-cyanovaleric acid) (ACVA), *N*-(*tert*-butoxycarbonyl)-ethylenediamine (Boc-EDA), copper(II) sulfate pentahydrate, 2-cyano-2-propyl benzodithioate, 4-cyano-4-thiobenzoylsulfanyl pentanoic acid (CTP), dicyclohexylcarbodiimide (DCC), *N,N*′-diisopropylethylamine

(DIPEA), *N*-(3-dimethylaminopropyl)-*N*′-ethylcarbodiimide hydrochloride (EDC), 4-(dimethylamino)pyridine (DMAP), *N*-ethylmaleimide (EtMI), methacrylic acid, methacryloyl chloride, poly(propylene glycol) triol (Mr 4800), propargylamine, sodium ascorbate, 4,5-dihydrothiazole-2-thiol (TT), triethylamine, tris[(1-benzyl-1H-1,2,3-triazol-4-yl)methyl]amine (TBTA) and 2,4,6-trinitrobenzenesulfonic acid solution (1 M in H_2O) were purchased from Sigma-Aldrich, UK. *N*-(2-Aminoethyl)methacrylamide hydrochloride was obtained from Polysciences, PA, USA. 2-[(*tert*-Butoxycarbonyl)amino]-3-cyanopropanoic acid dicyclohexylammonium salt (Boc-PGGly·DCHA) was purchased from Anaspec, CA, USA. Atto-488 NHS-ester fluorescent label was purchased from ATTO-TEC, Germany. All solvents used in this work were HPLC grade and purchased from Fisher Scientific, UK. Imiquimod, R848, HEK-Blue™-hTLR7 cell line, Blasticidin, Zeocin™, Normocin™ and QUANTI-Blue™ alkaline phosphatase detection reagent were obtained from InvivoGen, CA, USA. Human IL-6 and IP-10 ELISA kits were purchased from R&D Systems, MN, USA.

Synthesis of monomers

N-(2-Hydroxypropyl)methacrylamide (HPMA) was synthesized by reacting methacryloyl chloride with (RS)-1-aminopropan-2-ol in dichloromethane in the presence of sodium carbonate as described in[49].

N-[2-(tert-Butyloxycarbonyl)aminoethyl]methacrylamide (Boc-AEMA) was synthesized by the reaction of methacryloyl chloride with *N*-Boc-ethylenediamine in chloroform in the presence of triethylamine according to [50].

3-(6-Methacrylamidohexanoyl)thiazolidine-2-thione (Ma-ε-Ahx-TT) was synthesized by the Schotten–Baumann acylation of ε-Ahx with methacryloyl chloride in an aqueous alkaline medium followed by the reaction of formed 6-methacrylamidohexanoic acid with TT in tetrahydrofuran in the presence of DCC and DMAP as described in [51].

N-Propargylmethacrylamide (PGMA) was synthesized by reacting methacrylic acid with propargylamine in dichloromethane (DCM) in the presence of EDC. A mixture of methacrylic acid (1.567 g, 18.2 mmol) and EDC (4.525 g, 23.6 mmol) was dissolved in 86 mL of DCM and cooled to -18 °C. Propargylamine (1,0 g, 18,2 mmol) and a few crystals of DMAP were added to the cooled solution and the reaction mixture was

stirred 2 h at -18 °C and then overnight at r.t. The DCM solution was washed with brine (3 × 100 mL) and the organic layer was dried over anhydrous $MgSO_4$. After filtration of $MgSO_4$, the DCM solution was concentrated under reduced pressure and the product was isolated by crystallization from DCM/hexane/diethyl ether mixture. The yield was 1.23 g (55 %). The purity of the product was checked by reversed-phase HPLC, which showed a single peak with a retention time of 4.0 min (UV detection at 230 nm).1H-NMR (300 MHz, DMSO) δppm: 1.85 (s, 3H, -CH3), 3.05 (s, 1H, ≡CH), 3.88 (d, 2H, -CH2-), 5.37 and 5.68 (s, 1H, =CH2), 8.37 (s, 1H, -NH-).

tert-Butyl [1-({2-[(2-methacryloyl)amino]ethyl}amino)-1-oxopent-4-yn-2-yl]carbamate (Boc-PGGly-AEMA) was prepared by the condensation reaction of 2-[(*tert*-butoxycarbonyl)amino]pent-4-ynoic acid (Boc-PGGly) with *N*-(2-aminoethyl)methacrylamide hydrochloride (AEMA) in dichloromethane in the presence of DIPEA, EDC and DMAP. Boc-PGGly·DCHA (0.5 g, 1.3 mmol) was dissolved in 5 mL of aqueous $KHSO_4$ (1.9 mmol) and washed with ethyl acetate (3 × 5 mL). The combined organic portions were further washed with distilled water (3 × 5 mL) and dried over

anhydrous $MgSO_4$. After filtration of $MgSO_4$, ethyl acetate was evaporated off under reduced pressure yielding 0.287 g of the Boc-PGGly in the carboxylic acid form. A mixture of AEMA (0.244 mg, 1.5 mmol) and DIPEA (516 µL, 3.0 mmol) was suspended in 5 mL of DCM and added to a cooled solution (-18 °C) of Boc-PGGly (0.287 g, 1.4 mmol) and EDC (0.284 g, 1.5 mmol) in 5 mL of DCM. The reaction mixture was stirred 2 h at -18 °C and then overnight at r.t. After that, the DCM solution was sequentially washed with aqueous 1 M $KHSO_4$ (3 × 10 mL), 1 M NaCl (2 × 10 mL) and distilled water (1 × 10 mL). The organic layer was dried over anhydrous $MgSO_4$, followed by filtration and solvent evaporation. The product was isolated by crystallization from ethyl acetate/hexane mixture. The yield was 190.2 mg (43.6 %). The purity of the product was checked by reversed-phase HPLC, which showed a single peak with a retention time of 7.3 min (UV detection at 230 nm).1H-NMR (300 MHz, methanol) δppm: 1.44 (s, 9H, -C(CH3)3), 1.92 (s, 3H, -CH3), 2.34 (s, 1H, ≡CH), 2.47 - 2.67 (m, 2H, -CH2-C≡), 3.28 and 3.34 (t, 2H, -CH2-NH-), 4.14 (m, 1H, -CH-), 5.36 and 5.71 (s, 1H, =CH2).

Synthesis of PPG-based macro chain transfer agent (PPG-$(CTP)_3$)

A mixture of poly(propylene glycol) triol (0.100 g, 54.2 μmol) and EDC (0.102 g, 0.53 mmol) was dissolved in 10 mL of DCM, cooled to -18 °C and added to a cooled solution (-18 °C) of 4-cyano-4-thiobenzoylsulfanyl pentanoic acid (0.151 g, 0.54 μmol) in 5 mL of DCM. After that, a few crystals of DMAP were added to the reaction mixture and the solution was stirred 2 h at -18 °C and then overnight at r.t. The DCM solution was washed with brine (3 × 30 mL) and the organic layer was dried over anhydrous $MgSO_4$. After filtration of $MgSO_4$, the DCM solution was evaporated off under reduced pressure, the oily residue was dissolved in methanol and the crude product was purified by GPC using the Sephadex™ LH-20 (GE Healthcare Life Sciences, UK) in methanol. Methanol was removed under reduced pressure yielding 189.6 mg of the oily liquid. The content of DTB end groups was 0.51 mmol/g corresponding to ~2.6 DTB groups/PPG chain.

Synthesis of the Toll-like receptor 7/8 agonists

1-(4-[[(5-Azidopentanoyl)amino]methyl]phenyl))-2-butyl-1H-imidazo[4,5-c]quinolin-4-amine (2BXy-N3) and 1-(4-(aminomethyl)benzyl)-2-butyl-1H-imidazo[4,5-c]quinolin-4-

amine (2BXy-NH_2) were prepared by the multistep synthesis starting from quinolone - 2,4-diol as described elsewhere[21, 48].

Synthesis of the mannose-derived targeting unit

2-Imino-2-methoxyethyl-1-thiomannose (Man-IME) was prepared by multistep modification of mannose as described in [52].

Synthesis of polymer precursors

Statistical ter-polymer P[(HPMA)-*co*-(PGMA)-*co*-(AEMA)] (PP1) was synthesized by reacting HPMA, PGMA and Boc-AEMA in the presence of ACVA as an initiator and CTP as a RAFT agent (Supplementary Scheme S1). A mixture of ACVA (1.3 mg, 4.7 μmol) and CTP (2.6 mg, 9.3 μmol) was dissolved in 0.65 mL of dioxane and added to a solution of HPMA (250.0 mg, 1.75 mmol), PGMA (12.0 mg, 97.0 μmol) and Boc-AEMA (22.1 mg, 97.0 μmol) in 1.29 mL of H_2O. The reaction mixture was thoroughly bubbled with Ar and polymerized at 70 °C for 7 h. The polymer was isolated by precipitation to acetone followed by re-precipitation from methanol to acetone/diethyl ether mixture (3:1). The yield was 164.8 mg of pink powder. Crystalline $NaBH_4$ (20.8 mg, 0.55 mmol)

was added to the solution of the polymer (164.8 mg, 5.5 μmol DTB) in 1.8 mL of methanol and the reaction mixture was shaken for ~1 h until the pink solution become decolorized. After that, EtMI (13.7 mg, 0.11 mmol) was added to the solution and the mixture was shaken for next 2 h. The low-molecular-weight impurities were removed from the polymer solution by GPC using Sephadex™ LH-20 in methanol. Methanol was removed under reduced pressure; the residue was dissolved in 2.0 mL of 3M HCl/methanol mixture and allowed to incubate overnight. The solvent was evaporated to dryness; the polymer was re-dissolved in methanol and precipitated to diethyl ether yielding 148.2 mg of white powder. The molecular weight characteristics of the polymer precursor PP1 are stated in Supplementary Table S1.

Statistical co-polymer P[(HPMA)-*co*-(PGGly-AEMA)] (PP2) was synthesized by copolymerizing HPMA and Boc-PGGly-AEMA in the presence of ACVA as an initiator and CTP as a RAFT agent (Supplementary Scheme S2). A mixture of ACVA (1.3 mg, 4.7 μmol) and CTP (2.6 mg, 9.3 μmol) was dissolved in 0.61 mL of dioxane and added to a solution of HPMA (250.0 mg, 1.75 mmol) and Boc-PGGly-AEMA (29.7 mg, 91.9

μmol) in 1.23 mL of H_2O. The reaction mixture was thoroughly bubbled with Ar and polymerized at 70 °C for 7 h. The polymer was isolated by precipitation to acetone followed by re-precipitation from methanol to acetone/diethyl ether mixture(3:1). The yield was 176.9 mg of pink powder. Crystalline $NaBH_4$ (22.3 mg, 0.59 mmol) was added to the solution of the polymer (176.9 mg, 5.9 μmol DTB) in 1.8 mL of methanol and the reaction mixture was shaken for ~1 h until the pink solution become decolorized. After that, EtMI (14.8 mg, 0.12 mmol) was added to the solution and the mixture was shaken for 2 h. The low-molecular-weight impurities were removed from the polymer solution by GPC using Sephadex™ LH-20 in methanol. Methanol was removed under reduced pressure; the residue was dissolved in 2.0 mL of 3M HCl/methanol mixture and allowed to incubate overnight. The solvent was evaporated to dryness; the polymer was re-dissolved in methanol and precipitated to diethyl ether yielding 169.1 mg of white powder. The molecular weight characteristics of the polymer precursor PP2 are stated in Supplementary Table S1.

Di-block co-polymer P[(HPMA)-*co*-(PGMA)]-*b*-P[(HPMA)-*co*-(AEMA)] (PP3) was produced in two synthetic steps. First, the P[(HPMA)-*co*-(PGMA)] block was synthesized by copolymerizing HPMA and PGMA using ACVA as an initiator and CTP as a RAFT agent. Next, the initial block was used as a macro-RAFT agent and subjected to a chain extension polymerization with HPMA and Boc-AEMA in the presence of ACVA (Supplementary Scheme S3). A mixture of ACVA (7.3 mg, 25.9 μmol) and CTP (14.5 mg, 51.7 μmol) was dissolved in 2.59 mL of dioxane and added to a solution of HPMA (1.0 g, 6.98 mmol) and PGMA (95.6 mg, 0.78 mmol) in 5.17 mL of H_2O. The reaction mixture was thoroughly bubbled with Ar and polymerized at 70 °C for 7 h. The polymer was isolated by precipitation to acetone followed by re-precipitation from methanol to acetone/diethyl ether mixture (3:1). The yield was 550.0 mg of P[(HPMA)-*co*-(PGMA)] in the form of pink powder. The molecular weight characteristics of the polymer precursor were: M_w = 18 000 g/mol, M_n = 15 200 g/mol and M_w/M_n = 1.19. The content of DTB end groups was 0.65 mmol/g corresponding to ~0.99 DTB groups/polymer chain. Next, a mixture of HPMA (63.1 mg, 0.44 mmol), Boc-AEMA (11.2 mg, 0.49 μmol), P[(HPMA)-*co*-(PGMA)] (50.0 mg, 3.26 μmol DTB groups) and ACVA

(0.18 mg, 0.65 μmol) were dissolved in 0.33 mL of dioxane/H_2O mixture (2:1), thoroughly bubbled with Ar and polymerized at 70 °C for 16 h. The diblock copolymer was isolated by precipitation to acetone yielding 74.7 mg of pale pink powder. Crystalline $NaBH_4$ (6.2 mg, 0.17 mmol) was added to the solution of the polymer (74.7 mg, 1.7 μmol DTB groups) in 1.0 mL of methanol and the reaction mixture was shaken for ~1 h until the pink solution become decolorized. After that, EtMI (4.1 mg, 33.0 μmol) was added to the solution and the mixture was shaken for next 2 h. The low-molecular-weight impurities were removed from the polymer by GPC using Sephadex™ LH-20 in methanol. Methanol was removed under reduced pressure; the residue was dissolved in 1.0 mL of 3M HCl/methanol mixture and allowed to incubate overnight. The solvent was evaporated to dryness, the polymer was re-dissolved in methanol and precipitated to diethyl ether yielding 65.7 mg of white powder. The molecular weight characteristics of the polymer precursor PP3 are stated in Supplementary Table S1.

Multiblock co-polymer PPG-*b*-P[(HPMA)-*co*-(PGMA)-*co*-(AEMA)] (PP4) was synthesized by copolymerizing HPMA, PGMA and Boc-AEMA in the presence of

azobisisobutyronitrile (AIBN) as an initiator and PPG-$(CTP)_3$ (for the synthesis see above) as a trifunctional macro-RAFT agent. A mixture of HPMA (198.4 mg, 1.39 mmol), PGMA (9.5 mg, 77.0 μmol), Boc-AEMA (17.6 mg, 77.0 μmol), AIBN (0.4 mg, 2.57 μmol) and PPG-$(CTP)_3$ (10.0 mg, 5.13 μmol) were dissolved in 3,08 mL of *tert*-butanol, thoroughly bubbled with Ar and allowed to polymerize at 70 °C for 18 h. The product was isolated by precipitation to diethyl ether and purified by GPC using Sephadex™ LH-20 in methanol. The purified polymer was precipitated to diethyl ether yielding 66.1 mg of pink powder. Crystalline $NaBH_4$ (3.8 mg, 101.4 μmol) was added to the solution of the polymer (66.1 mg, 1.0 μmol DTB) in 661 μL of methanol and the reaction mixture was shaken for ~1 h until the pink solution become decolorized. After that, EtMI (2.5 mg, 20.3 μmol) was added to the solution and the mixture was shaken for 2 h. The low-molecular-weight impurities were removed from the polymer by GPC using the Sephadex™ LH-20 in methanol. Methanol was removed under reduced pressure; the residue was dissolved in 1.0 mL of 3M HCl/methanol mixture and allowed to incubate overnight. The solvent was evaporated to dryness; the polymer was re-dissolved in methanol and precipitated to diethyl ether yielding 40.0 mg of white powder.

The molecular weight characteristics of the polymer precursor PP4 are summarized in Supplementary Table S1.

Statistical co-polymer p[(HPMA)-*co*-(Ma-ε-Ahx-TT)] (PP5) was synthesized by copolymerizing HPMA and Ma-ε-Ahx-TT using the free radical polymerization technique as described elsewhere [21]. Briefly, a mixture of HPMA (9.8 wt%), 2-Methyl-N-[6-oxo-6-(2-thioxo-thiazolidin-3-yl)-hexyl]-acrylamide (Ma-ε-Ahx-TT) (5.2 wt%) and AIBN (1.5 wt%) were dissolved in DMSO (83.5 wt%) and polymerized at 60°C for 6 hours under argon atmosphere. The polymer was precipitated from a 1:1 mixture of acetone and diethyl ether and then dissolved in methanol and precipitated from a 3:1 mixture of acetone and diethyl ether. The content of TT reactive groups determined by UV-Vis spectrophotometry was 14.8 mol% (ε^{305} =10,300 L/mol); the weight- and number-average molecular weights determined by size exclusion chromatography (SEC) were M_w = 31,850 g/mol and M_n = 20,330 g/mol, respectively. The molecular weight characteristics of the polymer precursor PP5 are summarized in Supplementary Table S1.

Synthesis of polymer-TLR-7/8a conjugates

Polymer-TLR-7/8a conjugates, with the exception of conjugate PC13, were synthesized using azide-alkyne Huisgen cycloaddition to react the polymer-bound propargyl groups with the azide group-functionalized agonist (2BXy-N_3) in the presence of copper catalyst (for conjugate structures see Figure 1; for reaction schemes see Supplementary Scheme S1 – S3). 10 mg of polymer precursors PP1 – PP4 were dissolved in the mixture of TBTA (3.52 μmol; 20 μL of 76.51 mg/mL stock solution in DMF), sodium ascorbate (3.52 μmol; 20 μL of 68.57 mg/mL stock solution in water) and 2BXy-N3 (0.70 μmol for PC1, PC4, PC7 and PC10, 1.76 μmol for PC2, PC5, PC8 and PC11 and 3.52 μmol for PC3, PC6, PC9 and PC12; corresponding to 8, 20 or 40 μL of 42.69 mg/mL stock solution in DMF) in a total volume of 100 μL of DMF and 80 μL of water. The solution was thoroughly bubbled with Ar and mixed with a solution of $CuSO_4$ (3.52 μmol; 20 μL of 28.03 mg/mL stock solution in water bubbled by Ar). The reaction mixture was briefly bubbled with Ar again and allowed to shake for 24 h at r.t. Afterwards, 1.8 mL of phosphate saline buffer containing 15 wt% of EDTA was added and the polymer

product was isolated by gel filtration using Sephadex™ PD-10 columns with water and as an eluent. The collected polymer fractions were freeze-dried. The molecular weight characteristics of the polymer-TLR-7/8a conjugates PC1 – PC12 are summarized in Supplementary Table S1.

Conjugate PC13 was synthesized by the acylation reaction of the polymer-bound TT groups (PP5) with amino group-functionalized agonist (2BXy-PEG4-NH_2) according to the procedure described in[21]. The molecular weight characteristics of the PC13 conjugate as well as the content of bound 2BXy are summarized in Supplementary Table S1.

Synthesis of mannose-targeted polymer-TLR-7/8a conjugates

The polymer-TLR-7/8a conjugates with the highest content of TLR-7/8a were also prepared with a mannose targeting unit to yield targeted polymer conjugates, TPC3, TPC9 and TPC12, which were produced by the polymer-analogous reaction of the polymer-bound primary amino groups with an imidoester derivative of mannose (Man-IME, for conjugate structures see Figure 1; for reaction schemes see Supplementary

Scheme S1 – S3). 5 mg of polymer conjugates PC3, PC9 and PC12 were dissolved in 100 μL of phosphate saline buffer at pH 8.0 and thoroughly bubbled by Ar. The solution of Man-IME (4.7 mg, 17.6 μmol - ten molar excess related to amino groups) in 100 μL of the buffer was added to the polymer solution. The reaction mixture was bubbled by Ar for 5 min and shaken for 24 h at r.t. Polymer conjugates were purified by gel filtration using Sephadex™ PD-10 column with water as an eluent and isolated by freeze-drying. The molecular weight characteristics of the mannose-targeted polymer-TLR-7/8a conjugates TPC3, TPC9 and TPC12 are summarized in Supplementary Table S1.

Size-exclusion chromatography (SEC)

The molecular weights and molecular weights distributions of the polymers were determined by SEC on a HPLC system (Shimadzu VP, Japan) equipped with internal UV–VIS, and external RI, dual LS and viscometric detectors (Agilent Technologies, CA, USA). TSK-Gel SuperAW4000 column (6.0 × 150 mm, Tosoh Bioscience, Japan) and 80 % methanol / 20 % sodium acetate buffer (0.3 M, pH 6.5) mixture as a mobile phase (flow rate 0.6 mL/min) were used in all experiments. A method based on the known total

injected mass with an assumption of 100 % recovery was used for the calculation of the refractive index increments (dn/dc) needed for the molecular weights determination from light scattering data.

High-performance liquid chromatography (HPLC)

The purity of synthesized monomers and other low-molecular-weight reagents were determined by liquid chromatography on a HPLC system (Shimadzu Nextera, Japan) using a reversed-phase column Chromolith RP18-e (4.6 × 100 mm, Merck, Germany), with a linear gradient (0 − 100 %) of water/acetonitrile mixture containing 0.1% TFA at a flow rate 1.0 mL/min and a UV-VIS photodiode array detector (Shimadzu, Japan).

Determination of small molecule TLR-7/8a pharmacokinetics using UPLC-MS/MS

UPLC-tandem mass spectrometry (UPLC-MS/MS) methods were developed to determine 2BXy and R848 concentrations in mouse blood, spleen and lymph node samples. Mass spectrometric analysis was performed on a Waters Xevo TQ-S triple quadrupole instrument using electrospray ionization in positive mode with selected reaction monitoring (SRM). The SRM for 2BXy and R848 was 360.1/241 and 315.2/197,

respectively. The separation was performed using an Acquity BEH C18 column (50 x 2.1 mm, 1.7 μ) and a Waters Acquity UPLC system with 0.6 mL/min flow rate. The column temperature was maintained at 60°C. The mobile phase A was 0.1% formic acid in 10%MeOH/water and the mobile phase B was 0.1% formic acid in acetonitrile. The calibration standards (0.5 -1000 ng/mL for 2BXy and 0.05-500 ng/mL for R848) were prepared in the control blood and tissue homogenates from untreated animals. 10 μL blood sample or 40 μL of tissue homogenate was mixed with 200 μL internal standard in acetonitrile to precipitate proteins in a 96-well plate. 1.0 μL supernatant was injected for HPLC-MS/MS analysis. Pharmacokinetic parameters were calculated using WinNonlin V6.4.

UV-VIS spectrophotometry

The spectrophotometric analyses of the polymers were carried out in quartz glass cuvettes on a UV-VIS spectrophotometer Shimadzu UV-mini 1240 (Shimadzu, Japan). The content of dithiobenzoate (DTB) end groups in the polymers were determined at 302 nm in methanol using the molar absorption coefficient ε^{302} (DTB) = 12,100

L/mol·cm. The functionality of the polymer (f, the amount of the functional end groups per one polymer chain) was defined as the ratio between M_n obtained from the SEC measurement and M_n calculated from the end group analysis. The content of primary amine groups in the polymers was determined using a standard TNBSA assay. The determination of the 2BXy ligand content in the polymer-TLR-7/8a conjugates was performed at 325 nm in methanol using the molar absorption coefficient ε^{325} (2BXy) = 5,012 L/mol·cm. The content of carbonylthiazolidine-2-thione (TT) reactive groups in the polymer precursor was determined at 305 nm using the molar absorption coefficient ε^{305} (TT) = 10,300 L/mol·cm.

Static light scattering (SLS)

SLS measurements were carried out with an ALV-Goniometer System (Model ALV / CGS-8F, ALV, Germany) equipped with a 30 mW 632.8 nm He–Ne laser in the angular range 40–150° in PBS buffer (pH 7.4). The weight-average molecular weight (M_w) and radius of gyration (R_g) were calculated using the Zimm plot procedure.

Dynamic light scattering (DLS)

The hydrodynamic radii (R_H) of the PPG-based multiblock polymers were measured by the DLS technique at a scattering angle θ = 173° in PBS buffer (pH 7.4) using a Nano-ZS instrument (Model ZEN3600, Malvern Instruments, UK) equipped with a 632.8 nm laser. For the evaluation of the dynamic light scattering data, the DTS(Nano) program was used. The resulting R_H values were arithmetic means of at least three independent measurements.

Flow cytometry

Samples were acquired on a modified LSR II flow cytometer (BD). Results were analyzed using FlowJo version 9.3, Pestle version 1.6.2, and SPICE version 5.22 software (Mario Roederer, Vaccine Research Center, National Institute of Allergy and Infectious Diseases, National Institutes of Health, Bethesda, MD).

Animals

C57BL/6 (B6), B6.129S1-*Il12b*^{tm1Jm}/J (IL-12p40 KO), B6.129S2-*Ifnar1*^{tm1Agt}/Mmjax (IFNαβR KO) and B6.129S4-*Ccr2*^{tm1Ifc}/J (CCR2 KO) mice were obtained from The Jackson Laboratory (Bar Harbor, ME) and maintained at the Vaccine Research Center's

Animal Care Facility under pathogen-free conditions. Wild type mice used in this study were female and between 8 and 12 weeks old at the start of experiments. Both male and female KO mice were used and were between 6 to 18 weeks old at the start of experiments.

Animal protocol

All animal experiments were conducted at the National Institutes of Health (Bethesda, MD) and were in compliance with the guidelines set by the Association for the Assessment and Accreditation of Laboratory Animal Care International (AAALAC) and the Institutional Animal Care and Use Committee (ACUC). All experimental animal protocols underwent review and were approved by the Vaccine Research Center ACUC prior to the start of experiments.

Immunizations

Vaccines were prepared in sterile, endotoxin-free (<0.05 EU/mL) PBS (Gibco, Life Technologies) and administered subcutaneously in a total volume of 50 μL. All immunogens were certified endotoxin free (<1 EU/mg) by the manufacturer or were

prepared in-house with <5 EU/mg as determined by LAL assay (Genscript, Piscataway, NJ). EndoFit Ovalbumin was obtained from Invivogen (San Diego, CA). Adjuvants had < 1EU/mg endotoxin and were produced by synthetic means and were not from animal or human origin. Vaccine grade R848 was obtained from Invivogen and all other adjuvants were produced in-house under sterile conditions.

Ex vivo lymph node cultures for cytokine determination

Proximal draining lymph nodes were harvested at various time points following subcutaneous administration of different adjuvants or controls in 50 µL PBS (pH 7.4). Lymph nodes were placed in 300 µL of RPMI supplemented with 10% (v/v) fetal calf serum, 50 U/ml penicillin, 50 µg/ml streptomycin and 2 mM L-glutamine in 1.5 mL DNase, RNase, Pyrogen free Kontes Pellet Pestle Grinders (Kimble-Chase, Vineland, NJ) sitting on ice. Lymph nodes were gently mechanically disrupted using sterile pestles and the resulting suspensions were vortexed for 5 seconds and added to a 96 well round bottom culture plate that was incubated at 37°C / 5% CO_2 for 8 h. Supernatant was collected and stored at -80°C until analyzed by ELISA.

Lymph node and serum cytokine measurements

Cytokines in lymph node culture supernatants and sera were determined using ELISA kits according to the manufacturer's recommended guidelines. ELISA kits for murine IL-12p40 and IP-10 were obtained from Peprotech (Rocky Hill, NJ). Concentrations of individual cytokines in the supernatants were determined from standard curves.

Analysis of innate immune cells from lymph nodes and spleen

The magnitude, activation status and adjuvant uptake of innate immune cells in popliteal lymph nodes were evaluated as previously described [23], with slight modifications. Briefly, popliteal lymph nodes from both hind legs of immunized mice were harvested and added to pestle tubes for mechanical disruption as described above. Resulting lymph node cell suspensions were spun down, supernatant was removed and cells were re-suspended in 1 mL of an enzyme cocktail comprised of 1 mg/ml collagenase D (Roche, Basel, Switzerland) and 100 U/mL recombinant DNase I (Roche) in RPMI for 30 minutes at 37°C. Lymph node cells were then washed and resuspended in PBS and added to 96 well plates for staining. Cells were stained with LIVE/DEAD cell stain

(Aqua, Life Technologies) for 10 minutes at room temperature. Without washing, cells were stained for 15 minutes with FcR-Block, anti-CD16/CD32 (clone 2.4G2, BD Biosciences, Franklin Lakes New Jersey), followed by the addition of Brilliant Violet (BV) 510-anti-CD3e (145-2C11, BD), BV421-anti-CD19 (1D3, BD), BV605-anti-Ly-6G (1A8, BD), BV786-anti-CD8 (53-6.7, BD), BV510-anti-NK-1.1 (PK136, BD), Cy7-PE-anti-B220 (RA3-6B2, BD), PE-anti-CD11c (HL3, BD), Ax700-anti-CD11b (M1/70, BioLegend, San Diego, CA), Cy5-PE-anti-F4/80 (BM8, eBioscience, San Diego, CA), and CF594-PE-anti-CD80 (16-10A1, BD). Following incubation in the antibody cocktail for 20 minutes, cells were washed with PBS, resuspended in 0.5% paraformaldehyde / PBS and then evaluated by flow cytometry.

Tetramer staining of CD8 T cells from whole blood

Tetramer+ CD8 T cell responses were characterized from whole blood. Briefly, ~ 200 µL whole blood was collected from immunized mice in heparinized 1.5 mL polypropylene tubes. Following red blood cell lysis using ACK Lysing buffer (Life Technologies), cells were washed with PBS and then added to 96 well plates for staining. Cells were stained

with the viability dye LIVE/DEAD Fixable Orange (OrViD, Life Technologies) for 10 minutes at room temperature. After washing, cells were stained for 15 minutes with PE-H2-Kb OVA (SIINFEKL) tetramer (Beckman Coulter, Brea, California). Fc-Block, anti-CD16/CD32 (clone 2.4G2, BD), was added for 10 minutes, followed by the addition of APC-Cy7-anti-CD8 (53-6.7, Biolegend), PE-Cy7-anti-CD62L (MEL-14, Abcam, Cambridge, England), eFluor-660-anti-CD127 (A7R34, eBioscience) and FITC-anti-KLRG1 (2F1, Southern Biotech, Birmingham, Alabama). After incubating for 20 minutes at room temperature, cells were washed and then incubated with Fix / Perm solution (BD) for 20 minutes at 4°C. After washing, cells were suspended in perm wash buffer containing PerCP-Cy5.5-anti-CD3 (145-2C11, BD) and incubated at 4°C for 30 minutes. Cells were washed and suspended in perm wash buffer and then evaluated by flow cytometry.

Statistics and graphs

Statistical analyses were done using Prism software (GraphPad) using one-way analysis of variance (ANOVA). Bonferroni correction was applied to correct for multiple

comparisons. Differences were found to be significant when P was less than 0.05 or 0.01, as indicated by single (*) or double asterisks (**), respectively. Most graphs were produced using Prism. Flow cytometry data was processed using FlowJo (Tree Star).

RESULTS

Synthesis of polymer-TLR-7/8a conjugates

To permit the evaluation of how polymer composition, chain architecture and hydrodynamic behavior impacts the adjuvant activity of covalently attached TLR-7/8a, three morphologically different polymer-TLR-7/8a conjugates with varying TLR-7/8a density were prepared: (1) linear statistical ter-polymers (PC1-3) and co-polymers (PC4-6) based on *N*-(2-hydroxypropyl)methacrylamide (HPMA) polymer chains linked to multiple TLR-7/8a randomly distributed along the backbone; (2) a linear di-block co-polymer (PC7-9) based on HPMA wherein TLR-7/8a are attached to one statistical co-polymer-forming block of the di-block polymer; and (3) a branched multi-block co-polymer (PC10-12) consisting of three HPMA-based polymer arms radiating from a hydrophobic poly(propylene glycol) (PPG) core wherein multiple TLR-7/8a are randomly distributed along the HPMA polymer arms (Figure 1).

While HPMA-based polymers are biocompatible and have been safely used in humans and animals without reported toxicity [53-55], a potential safety concern is that non-biodegradable hydrocarbon-based backbones with a molecular weight above the filtration limit of the kidney (~ 45 kDa [56]) could accumulate in the body with unknown effects. To reduce these concerns, controlled radical polymerization by reversible addition-fragmentation chain-transfer polymerization ("RAFT") [57, 58] was used to synthesize polymer precursors ("PP") with narrow

molecular weight distribution at a mean molecular weight below the renal filtration limit (Supplementary Table 1 and Supplementary Schemes S1-3).

The next step in the synthesis was the attachment of TLR-7/8a to the polymer precursors to generate polymer-TLR-7/8a conjugates ("PC") (Supplementary Schemes S1-3). An imidazoquinoline-based agonist, referred to herein as "2BXy," which is approximately 40-fold more potent (EC50 = 0.02 μM than the structurally related and commercially available analog, R848 (EC50 = 0.82 μM; see Supplementary Figure S1), was selected for attachment to the polymer precursors. To facilitate attachment to the polymer precursors, the 2BXy molecule was modified with an azide group through the N^1 position as previously described [38]. Multiple azide-functionalized 2BXy molecules were then attached to each of the different polymer precursors at different densities using Cu(I)-catalyzed cycloaddition [59] to generate polymer-TLR-7/8a conjugates of varying hydrodynamic properties (co-polymer, di-block co-polymer and multi-block co-polymer) with different densities of attached TLR-7/8a (Supplementary Table 1). With the exception of the multi-block co-polymer, the resulting molecular weights of the conjugates linearly increased in accordance with the number of TLR-7/8a molecules attached without the occurrence of molecular weight distribution broadening.

Importantly, by keeping the TLR-7/8a density below 7 mol. %, the hydrophobic TLR-7/8a had minimal impact on the hydrodynamic characteristics of the polymer-TLR-7/8a conjugates. Accordingly, polymer-TLR-7/8a conjugates based on the statistical co-polymer and di-block co-polymer architectures had $R_H \sim 4$ nm corresponding to a random coil structure in aqueous solutions, while the polymer-TLR-7/8a conjugates based on the multi-block co-polymer with a hydrophobic PPG core had $R_H \sim 10$ nm consistent with their assembly into micelles (Supplementary Figure S2).

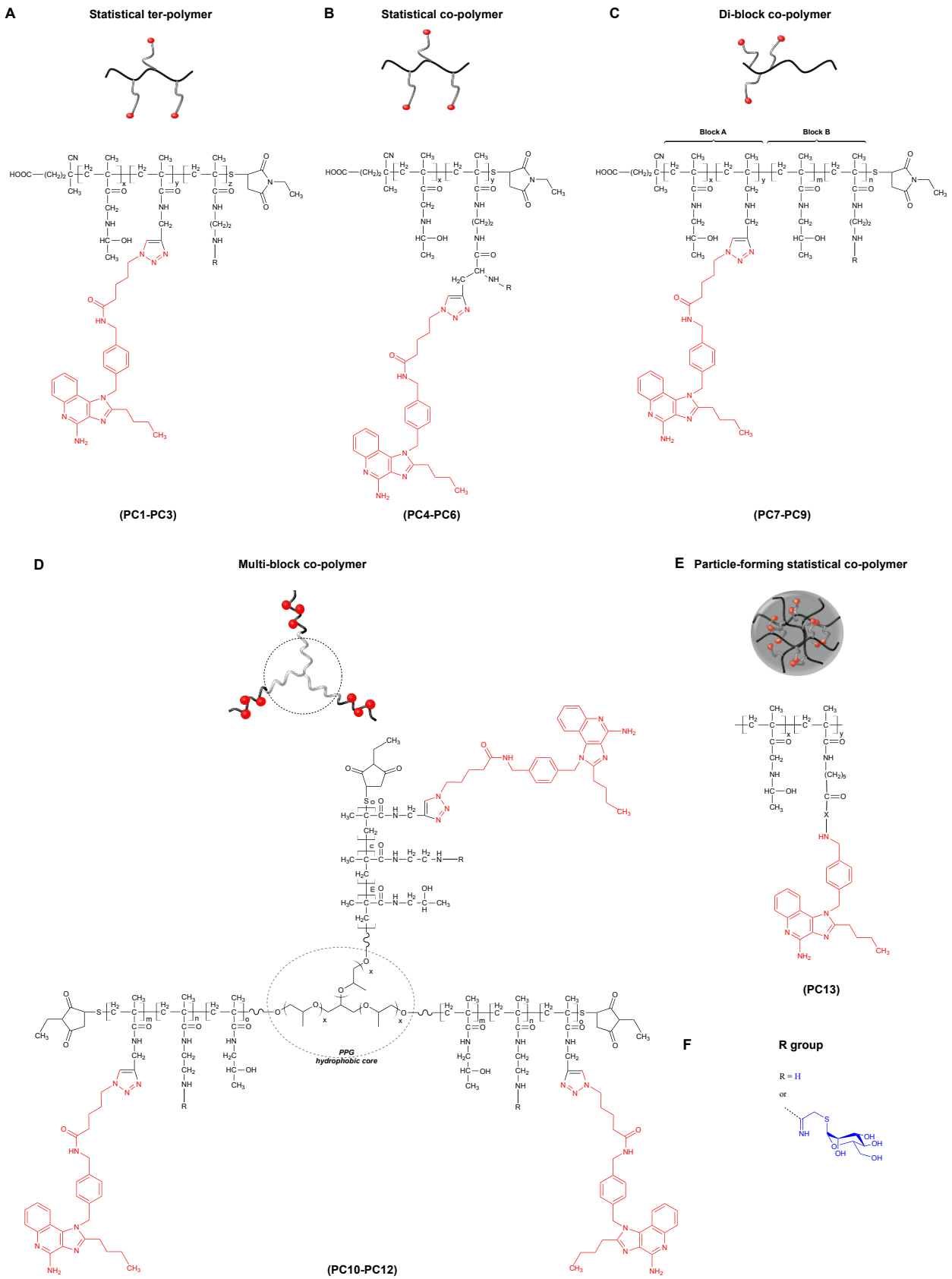
A
Statistical ter-polymer
B
Statistical co-polymer
C
Di-block co-polymer
Block A
Block B
(PC1-PC3)
(PC4-PC6)
(PC7-PC9)
D
Multi-block co-polymer
E
Particle-forming statistical co-polymer
(PC13)
PPG
hydrophobic core
(PC10-PC12)
F
R group
R = H
or

Figure 1. Polymer-TLR-7/8a conjugates (PC) prepared using the RAFT polymerization technique. Chemical structures and cartoon representations of the polymer-TLR-7/8a conjugates based on (A) statistical ter-polymers, PC1-PC3; (B) statistical co-polymers, PC4-PC6; (C) di-block co-polymers, PC7-PC9; (D) multi-block co-polymers, PC10-PC12; and, (E) particle-forming statistical co-polymer, PC13. (F) The "R" group was either mannose or hydrogen. X = PEG4.

Impact of agonist density and mannose targeting on polymer-TLR-7/8a conjugate adjuvant activity

The adjuvant activity of TLR-7/8a is in part mediated by the production of cytokines and chemokines (*e.g.*, IL-6, IL-12, IP-10 etc.) that influence the quality and magnitude of antibody and T cell responses [10]. Therefore, the capacity of the different polymer-TLR-7/8a conjugates to induce cytokines following incubation with human peripheral blood mononuclear cells (hPBMCs) was used to screen the different polymer-TLR-7/8a conjugate compositions for adjuvant activity *in vitro*. All of the polymer-TLR-7/8a conjugates induced >10-fold higher magnitude cytokine production (*i.e.* IP-10) compared with the polymer precursors without TLR-7/8a attached (Supplementary Figure S3). Additionally, there was a trend towards increasing magnitude of cytokine production with increasing densities of TLR-7/8a attached.

We next evaluated the impact that attachment of mannose to polymer-TLR-7/8a conjugates had on *in vivo* adjuvant activity. As polymer-TLR-7/8a must be internalized by APCs to access endosomally localized TLR-7 and TLR-8, we hypothesized that attachment of mannose units to the polymer-TLR-7/8a conjugates would improve their adjuvant activity by improving uptake by APCs through C-type lectin receptors (CLR) as has been observed for other mannose decorated particles [60, 61]. However, the mannose-targeted polymer conjugates provided no discernible

improvement in uptake by APCs or APC activation *in vivo* as compared with the non-targeted polymer conjugates (Supplementary Figure S4). As density [62] and saccharide composition [63, 64] are two factors that impact CLR binding on APCs, a potential explanation to account for these findings is that the density of mannose attached to the targeted polymer-TLR-7/8a conjugates evaluated herein may not have been sufficient to confer a benefit over the non-targeted conjugates. Thus, additional studies will likely be needed to determine the optimal composition and density of saccharides needed to confer improved APC targeting by polymer-TLR-7/8a conjugates.

Based on these data, the polymer-TLR-7/8a conjugates with the highest agonist density that do not display mannose were selected for further evaluation. Additionally, an HPMA-based polymer-TLR-7/8a conjugate that assembles into submicron particles (PC13, Supplementary Table S1) was prepared as previously described [21] and used herein to provide a broad range of different polymer-TLR-7/8a conjugate compositions for evaluating how hydrodynamic characteristics—random coil (PC03 and PC9), micelle nanoparticle (PC12) and submicron particle (PC13)—impact immune responses *in vivo*.

Impact of TLR-7/8a adjuvant composition and hydrodynamic behavior on CD8 T cell immunity

The efficiency of the different polymer-TLR-7/8a conjugate compositions for inducing CD8 T cells was assessed following their co-administration with the model antigen, Ovalbumin (OVA), which has been widely used in vaccine studies in mice. Mice were immunized with either polymer precursors ("PP"), small molecule TLR-7/8a or polymer-TLR-7/8a conjugates, each admixed with OVA protein.

Mice that received immunizations with polymer-TLR-7/8a conjugates had a >10-fold higher magnitude CD8 T cell response compared with mice that received OVA co-administered with the polymer precursors. Among the groups of mice that received the polymer-TLR-7/8a conjugates, there was a trend between increasing hydrodynamic radius and the magnitude of the resulting CD8 T cell response (Figure 2A). The submicron particle induced the highest magnitude response (~ 10% tetramer+ CD8 T cells), followed by the micelle-forming polymer and then random coil polymers (Figure 2A). These trends were also reflected in the efficiency of the different polymer-TLR-7/8a conjugates for inducing CD8 T cell responses over a range of doses evaluated *in vivo* (Figure 2B). Among the random coil-forming polymers, the single block copolymer (PC3) induced higher magnitude responses as compared with that of the di-block copolymer (PC9). Notably, the submicron particle polymer-TLR-7/8a, PC13, did not physically associate with the protein antigen (Supplementary Figure S5), which suggests that the increased CD8 T cell responses by the submicron particle are likely due to intrinsic properties of the adjuvant itself and not due to preferential association of PC13 with the antigen.

Among the small molecule TLR-7/8a evaluated, the unformulated small molecule TLR-7/8a, R848, induced no significant increase in CD8 T cell responses as compared with naïve, untreated mice (background). Unexpectedly, the small molecule TLR-7/8a, 2BXy, induced high magnitude CD8 T cell responses that were comparable to those induced by the polymer-TLR-7/8a conjugates (Figure 2A). However, modification of 2BXy with a short ethylene glycol linker ("PEG4") resulted in a nearly 5-fold decrease in CD8 T cell responses and a nearly 10-fold reduction in responses as compared with the same molecule, 2BXy-PEG4, linked to the submicron particle (PC13). Differences in adjuvant activity between 2BXy and 2BXy-PEG4 may be accounted for by the lower *in vitro* potency of 2BXy-PEG4 (EC50 = 5.48 μM) compared with

2BXy (EC50 = 0.02 μM) that could be due to interference of the PEG with receptor binding and/or reduced uptake of the PEG-modified agonist into endosomal compartments of APCs where TLR-7 is localized (Supplementary Figure S1). Despite the reduced *in vitro* activity due to modification with PEG, 2BXy-PEG4 linked to a submicron particle (PC13) led to the highest magnitude CD8 T cell responses *in vivo* (Fig. 2A), which suggests that improvements in the distribution, pharmacokinetics and/or cellular uptake by the carrier can offset reductions in *in vitro* potency that result from modifications used for conjugation (Supplementary Figure S1).

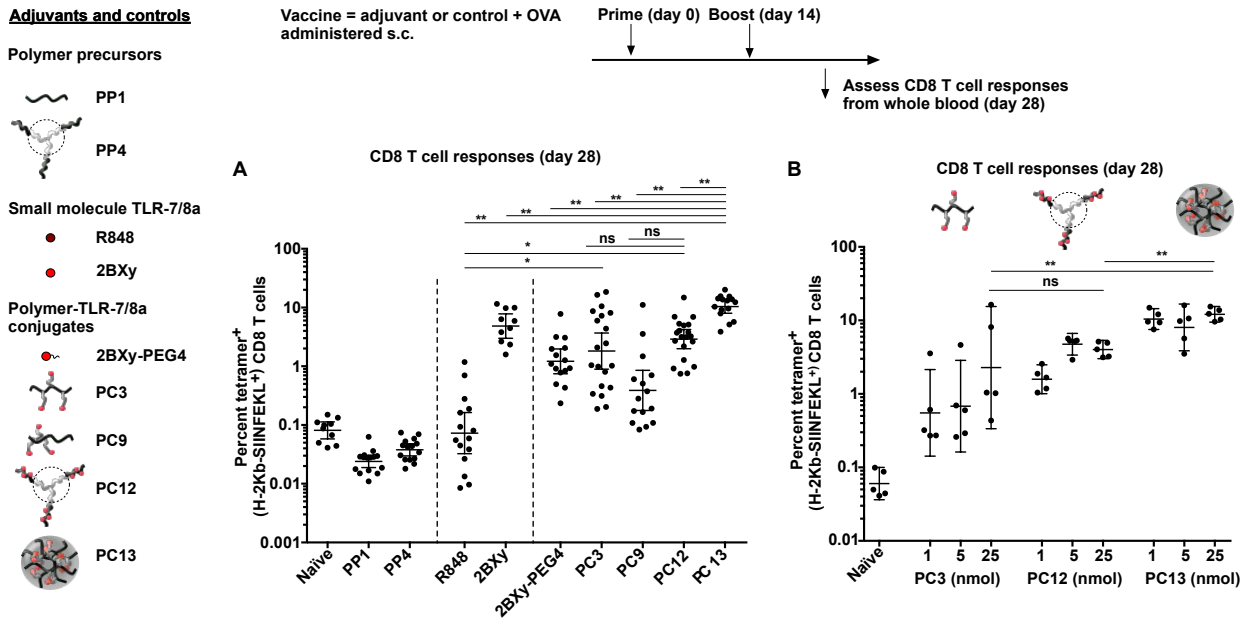

Figure 2. Impact of polymer-TLR-7/8a conjugate composition on CD8 T cell induction. Polymer precursors (PP), low-molecular-weight, small molecule TLR-7/8a and polymer-TLR-7/8a conjugates (PC) normalized for TLR-7/8a dose (25 nmol) were admixed with 50 μg of OVA in PBS and given subcutaneously to C57BL/6 mice at days 0 and 14. (A) Antigen-specific CD8 T cell responses were evaluated from whole blood of mice (n = 10-20) at day 28; responses shown are compiled from 3 independent studies. (B) In a separate study, CD8 T cell responses were assessed at day 28 from mice (n = 5) that received different doses of polymer-TLR-7/8a

conjugates (either 1, 5 or 25 nmol) admixed with 50 μg of OVA. Data are reported as geometric mean with 95% confidence interval (CI). Comparison of multiple groups for statistical significance was determined using one-way ANOVA with Bonferroni correction. Statistically significant responses are indicated by asterisks; *, p = 0.05; **, p = 0.01. PP = polymer precursor; PC = polymer conjugate.

Impact of TLR-7/8a adjuvant composition and hydrodynamic behavior on local and systemic cytokine production

The location of APC activation and cytokine production by TLR-7/8a in part determines the balance between adjuvant toxicity and efficacy. Accordingly, formulations that physically restrict TLR-7/8a to vaccine-site DLN have been shown to limit toxicity and are associated with enhanced T cell immunity [21, 41], while unformulated TLR-7/8a that enter the bloodstream cause systemic cytokine production that is associated with adjuvant toxicity and morbidity [17, 19, 20, 65]. To determine how polymer-TLR-7/8a conjugate composition impacts the balance between local and systemic cytokine and chemokine production, the concentration of IL-12p40 and IP-10 (CXCL10) were assessed from vaccine-site DLN and blood following subcutaneous administration of the different TLR-7/8a compositions. IL-12 and IP-10 were selected for evaluation because they are reliable biomarkers of TLR-7/8a adjuvant activity and are involved in the priming and expansion of CD8 T cells [11, 66, 67].

Among the polymer-TLR-7/8a conjugates, there was a direct correlation between hydrodynamic radius and the magnitude of lymph node IL-12 and IP-10 production (Figure 3A-D). The submicron particle (~ 300 nm) induced the highest lymph node cytokine production, followed by the nanoparticle micelle (~ 10 nm), random coil polymers (~ 4 nm) and 2BXy-PEG4 conjugate (~ 1 nm). Consistent with our prior findings [21], we observed that the polymer precursors and the

small molecule TLR-7/8a, R848, induced limited lymph node cytokine production. However, an unexpected finding was that the small molecule TLR-7/8a, 2BXy, selectively induced high magnitude IP-10 production (~ 100 pg/mL) that was comparable to that of the nanoparticle micelle and submicron particle polymer-TLR-7/8a conjugates (Figure 3B). As expected, the small molecule TLR-7/8 agonists, R848 and 2BXy, induced ~10-fold higher levels of systemic IL-12 and IP-10 at 4 hours (peak response in blood) as compared to the polymer-TLR-7/8a conjugates, which did not induce systemic cytokines significantly above background (Figure 3E & F).

These data substantiate that covalent linkage of TLR-7/8a to macromolecular carriers can mitigate systemic inflammation and show that the hydrodynamic size of the carrier is an important factor that influences the magnitude and composition of cytokines produced in DLN.

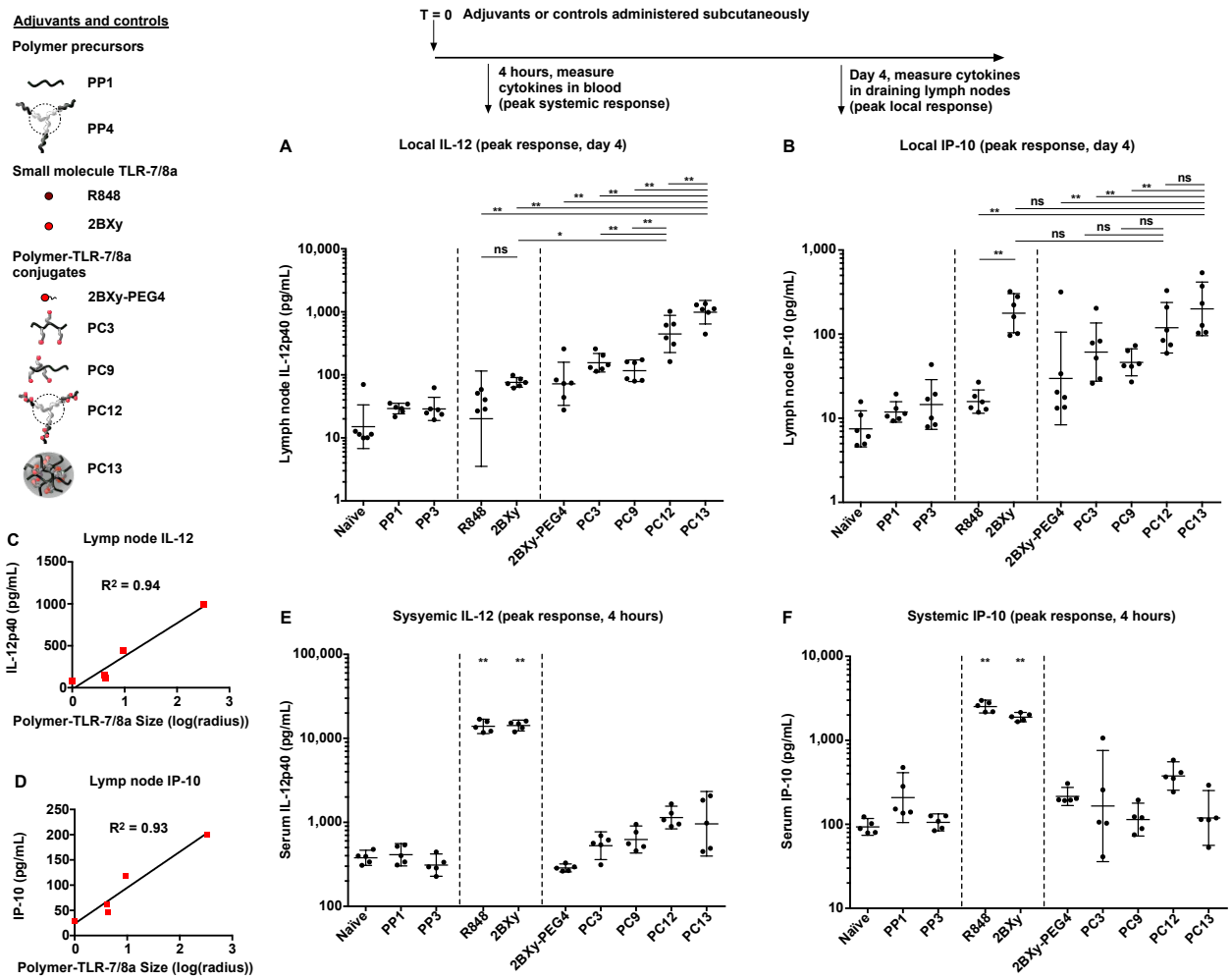

Figure 3. Impact of the TLR-7/8a composition and hydrodynamic behavior on local and systemic cytokine production. (A-F) Polymer precursors (PP), low-molecular-weight, small molecule TLR-7/8a and polymer-TLR-7/8a conjugates (PC) normalized for TLR-7/8a dose (25 nmol) were administered subcutaneously into the hind footpads of mice. Lymph nodes (n = 6) draining the site of administration were isolated on day 4 and the concentration of (A) IL-12p40 and (B) IP-10 from the supernatant of *ex vivo* lymph node cultures was determined by ELISA. Lymph node IL-12p40 (C) and IP-10 (D) concentrations at day 4 are plotted against the size (log(radius)) of the polymer-TLR-7/8a conjugates. Blood (n = 5 mice per group) was drawn 4 hours after administration of the adjuvants and evaluated for (E) IL-12p40 and (F) IP-10 by

ELISA. Data are reported as geometric mean with 95% CI. Comparison of multiple groups for statistical significance was determined using one-way ANOVA with Bonferroni correction. Unless otherwise indicated, statistical significance is indicated for groups as compared with naïve; *, p = 0.05; **, p = 0.01.

Pharmacokinetics of small molecule TLR-7/8a accounts for differences in adjuvant activity

Given the structural similarity between R848 and 2BXy, it was unexpected that 2BXy, but not R848, induced high magnitude CD8 T cell responses (Fig. 2A) and persistent IP-10 production in lymph nodes (Fig. 3B). To assess whether differences in pharmacokinetics could account for the observed differences in adjuvant activity, we quantified R848 and 2BXy levels in different tissues using ultra-performance liquid chromatography-tandem mass spectrometry (UPLC-MS/MS). Despite administering the same dose of each small molecule TLR-7/8a, the concentration of 2BXy was nearly 100-fold higher in all examined tissues (DLN, spleen and blood) and at all time points evaluated compared with R848 (Figure 4A & B and Supplementary Table 2 and 3). Such differences in tissue concentrations may be accounted for by different rates of clearance. Indeed, while clearance of both molecules from the blood was rapid ($T_{1/2}$ ~ 0.6 and 2 hours for R848 and 2BXy, respectively), the rate of clearance of 2BXy from DLN was ~15-fold slower ($T_{1/2}$ ~ 15 hours) than that of R848 ($T_{1/2}$ ~ 1.1 hours). Slower clearance resulted in concentrations of 2BXy exceeding the threshold required for immunological activity (*i.e.* EC50, Supplementary Figure S1) for up to 80 hours in the spleen, and for over 100 hours in the DLN. Notably, the onset of tissue swelling and resolution was concordant with the kinetics of 2BXy concentrations in each of the tissues examined (Figure 4C & D). Accordingly, spleen mass increased while the measured 2BXy concentration exceeded EC50 (> 0.02 μMolar) but resolved when concentrations of agonist dropped below EC50 (< 0.02 μMolar). Lymph node mass

continued to increase for up to 15 days following 2BXy administration, which may in part be accounted by our observation that 2BXy induced sustained production of chemokines (*i.e.* IP-10, Figure 3B) that attract immune cells to the inflamed tissue. The kinetics of cytokines in the blood was also concordant with the duration of time that the concentration of R848 and 2BXy remained above EC50. Blood cytokines induced by R848 and 2BXy were elevated at 4 hours but were no longer detectable after 24 hours when blood concentrations fell below EC50 (Figure 3E & F and Supplementary Figure S6).

These data suggest that differences in the *in vivo* PK between R848 and 2BXy likely account for differences in adjuvant activity. Accordingly, while unformulated R848 is rapidly eliminated and induces weak adjuvant activity in tissues (Fig. 3A & B), unformulated 2BXy rapidly distribute into the blood but is also unexpectedly retained in lymphoid tissues and leads to prolonged innate immune stimulation that is associated with robust induction of CD8 T cell immunity (Fig 2A).

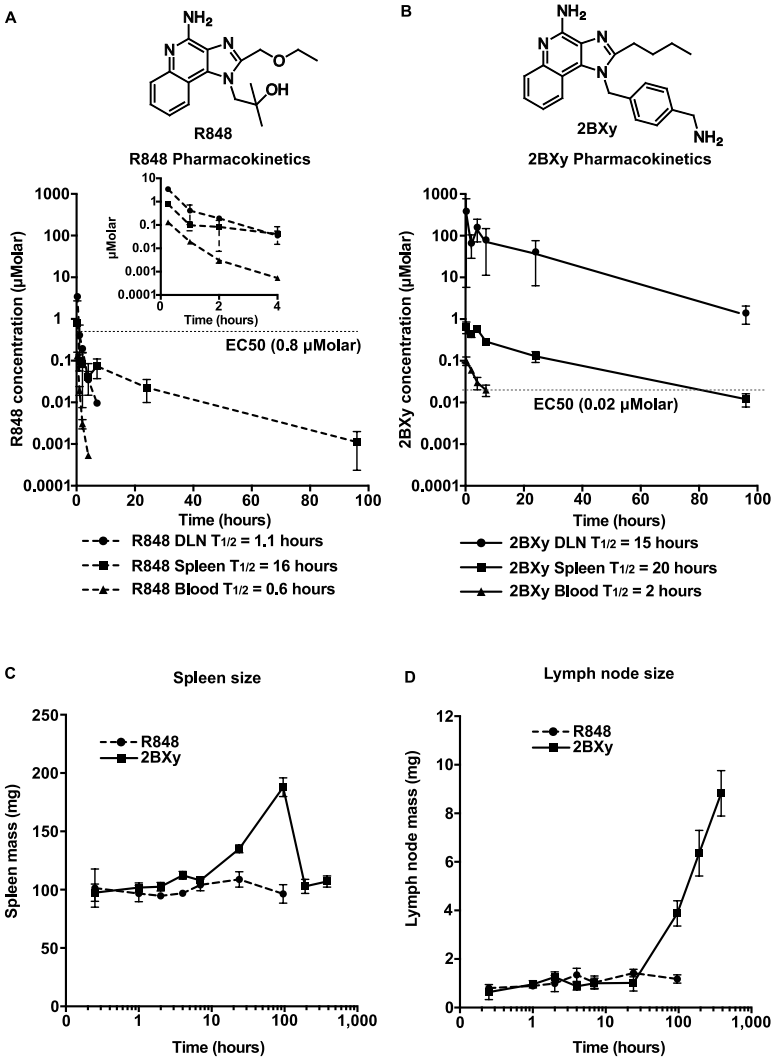

Figure 4. Pharmacokinetics account for differences in adjuvant activity between structurally related small molecule TLR-7/8a. (A-D) The low-molecular-weight, small molecule TLR-7/8a, R848 and 2BXy, were subcutaneously administered to mice (*n* = 3 per time point) at 25 nmol and then tissue was harvested at serial time points thereafter to evaluate concentrations of R848 (A) and 2BXy (B) in DLN, spleen and blood; the mass of spleen (C) and DLN (popliteal) (D) tissue were also assessed. Data are reported as mean ± standard error of the mean (SEM).

Influence of TLR-7/8a adjuvant composition and hydrodynamic behavior on APC recruitment, activation and polymer uptake

To investigate the innate mechanisms accounting for the observed differences in adjuvant activity, we assessed the recruitment of APCs to, and material uptake by APCs within, DLN following subcutaneous administration of the different TLR-7/8a compositions to mice.

While all of the polymer-TLR-7/8a compositions induced comparable magnitude of APC recruitment to DLN (Figure 5A & B), the submicron particle polymer-TLR-7/8a conjugate (PC13) had significantly higher levels of uptake by both monocytes/macrophages and DCs as compared with the micelle (PC12) and random coil (PC3) polymer-TLR-7/8a conjugates (Figure 5C & D). Notably, uptake of the submicron particle polymer-TLR-7/8a conjugate was about 5-fold higher for monocytes and macrophages as compared with uptake by DCs, suggesting that monocytes and/or macrophages may play a critical role in the adjuvant activity by the submicron particle polymer-TLR-7/8a. In contrast, the small molecule, 2BXy, promoted significantly higher accumulation of DCs in lymph nodes compared with the submicron particle (Figure 5A & B). Note: APC uptake was not assessed for the small molecule TLR-7/8a, 2BXy, as covalent attachment of a ~ 1,000 Da fluorophore would likely confound results.

IL-12 production by submicron particle polymer-TLR7/8a conjugates requires CCR2+ monocytes

It has been recognized recently that monocytes can play a role in promoting T cell immunity through antigen presentation and the production of inflammatory cytokines [68,69, 70]. While the role of monocytes in adaptive immunity is highly context dependent, it remains unknown how different formulations of the same innate stimulus (*e.g.,* TLR-7/8a) impact monocyte involvement. Therefore, to evaluate a possible mechanistic role of monocytes in the adjuvant

activity of the different TLR-7/8a compositions, we utilized chemokine receptor-2 deficient (CCR2 KO) mice. In these mice, monocytes are unable to efficiently exit the bone marrow and enter inflamed tissues but other immune cell populations are intact and fully functional [68, 71].

CCR2 KO mice vaccinated with the submicron particle polymer-TLR-7/8a conjugate had significantly fewer monocytes in the DLN as compared with wild type (WT) mice (Fig. 5E). Notably, WT and CCR2 KO mice had a similar magnitude of resident and migratory DCs in DLN following vaccination with either the submicron particle polymer-TLR-7/8a or the small molecule TLR-7/8a, 2BXy (Fig. 5F). These data substantiate that CCR2 KO mice are suitable for assessing the role of monocytes in DLN and that CCR2 deficiency does not affect recruitment of other APCs to DLN.

To further investigate a potential mechanistic role of monocytes in the adjuvant activity by the submicron particle polymer-TLR-7/8a conjugate, we assessed IL-12 production from the DLN of CCR2 KO mice. These studies were motivated in part by recent work by De Koker *et al* showing that the adjuvant activity of a TLR-9a (CpG) depends on monocyte production of IL-12 [70]. Consistent with this reported role of monocytes, we observed that the absence of monocytes in CCR2 KO mice vaccinated with the submicron particle polymer-TLR-7/8a was associated with a significant decrease in IL-12 on day 1 and a nearly 5-fold reduction in DLN IL-12 at peak response (day 4) as compared to WT mice (Figure 5G). In contrast, no significant difference in IL-12 production was observed for WT and CCR2 KO mice that received the small molecule TLR-7/8a, 2BXy.

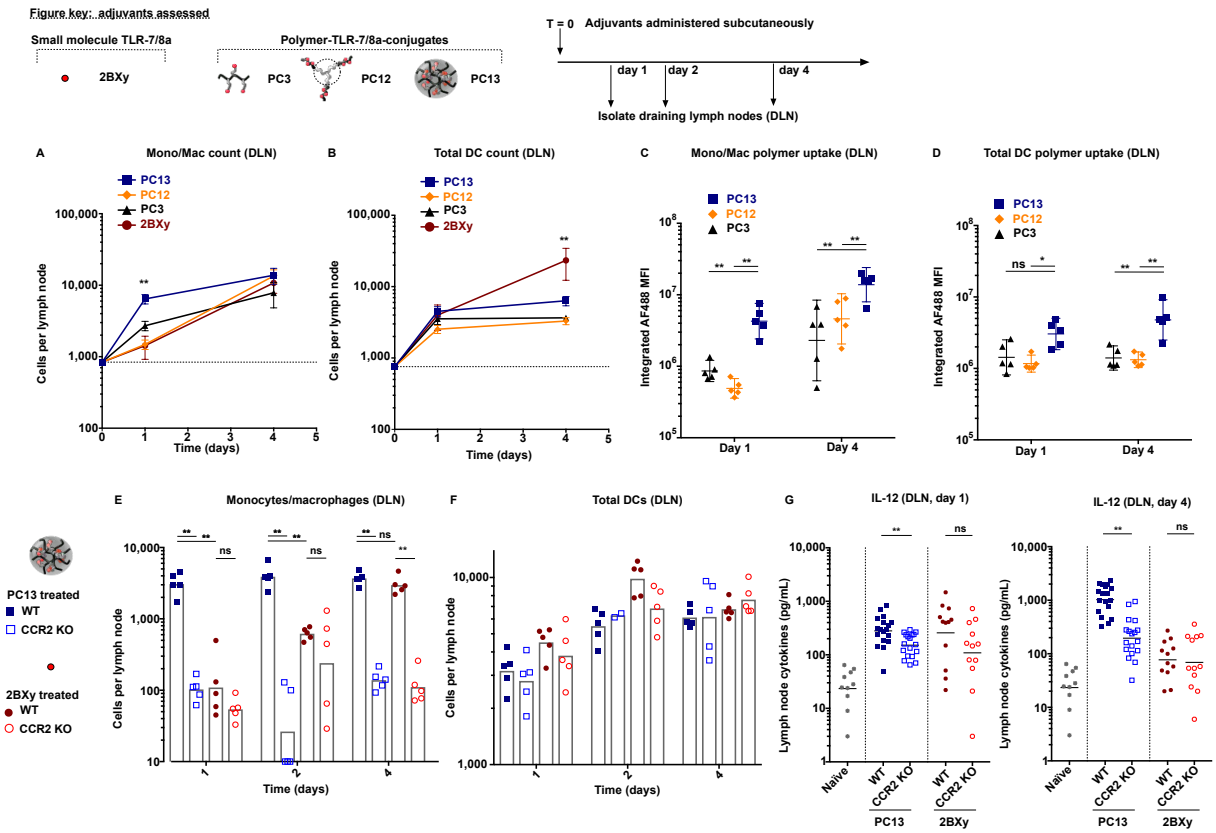

Figure 5. Robust IL-12 production by the submicron particle polymer-TLR-7/8a conjugate depends on CCR2+ monocyte recruitment to the DLN. (A-D) Mice received either a low-molecular-weight TLR-7/8a or a fluorophore-labeled polymer-TLR-7/8a conjugate (PC) normalized for TLR-7/8a dose (25 nmol) administered subcutaneously into the hind footpad. At serial timepoints thereafter, DLN (n = 5 per time point per group) were harvested and processed to generate cell suspensions that were evaluated by flow cytometry to enumerate the total number of monocytes/macrophages (defined as $CD11b^{+}Ly6c^{+}$ cells) (A) and DCs (defined as $Ly6c^{-}CD11c^{+}$ cells) (B), as well as polymer-TLR-7/8a conjugate uptake by monocytes/macrophages (C) and DCs (D) in DLN. (E-G) Wild type (WT) and CCR2 deficient (CCR2 KO) mice were immunized with either 2BXy or the submicron particle, polymer-TLR-7/8a conjugate, PC13, and DLN were isolated for evaluation at serial time points thereafter. DLN cell suspensions were stained and evaluated by flow cytometry to enumerate

monocytes/macrophages (E) and DCs (F). Lymph nodes (*n* = 10-18 per time point) draining the site of administration were isolated on days 1 and 4 and the concentration of IL-12p40 from the supernatant was determined by ELISA (G); results are compiled from 3 independent studies. Data on line graphs are reported as mean ± SEM. Data on log scale are reported as geometric mean or geometric mean with 95% CI. Comparison of multiple groups for statistical significance was determined using one-way ANOVA with Bonferroni correction. Unless otherwise indicated, statistical significance is indicated for groups as compared with naïve; ns = not significant; *, p = 0.05; **, p = 0.01.

CD8 T cell responses by the submicron particle polymer-TLR-7/8a conjugate depend on monocytes and IL-12

To further investigate the innate immune mechanisms responsible for the adjuvant activity of different compositions of TLR-7/8a, we evaluated CD8 T cell responses following vaccination of mice deficient in either monocyte recruitment to tissue (CCR2 KO), IFN signaling (IFNαβR KO) or IL-12 production (IL-12 KO) (Figure 6A-C). The dependence of CD8 T cell responses on IL-12 (Fig. 6A) closely mirrored the relative amounts of lymph node IL-12 elicited by each of the distinct TLR-7/8a formulations (Figure 3A). Moreover, while the magnitude of CD8 T cells induced by the submicron particle polymer-TLR-7/8a conjugate was reduced by about 10-fold in the IL-12 and CCR2 deficient mice as compared with WT mice, knocking out IL-12 or lymph node monocyte recruitment had only a modest impact on CD8 T cell responses in mice vaccinated with the small molecule TLR-7/8a, 2BXy (Figure 6B). As excepted, mice deficient for IFNα and IFNβ receptors (IFNαβR KO mice) had markedly reduced magnitude CD8 T cell responses when immunized with either the submicron particle or small molecule TLR-7/8a,

which substantiates the critical role of Type I IFNs in promoting CD8 T cell immunity to exogenously delivered antigen [72].

Altogether, these data show that different formulations of the same TLR-7/8a differentially require monocytes and IL-12 for promoting CD8 T cell immunity and reveal an important and novel role of monocytes in the adjuvant activity by polymer carriers of TLR-7/8a.

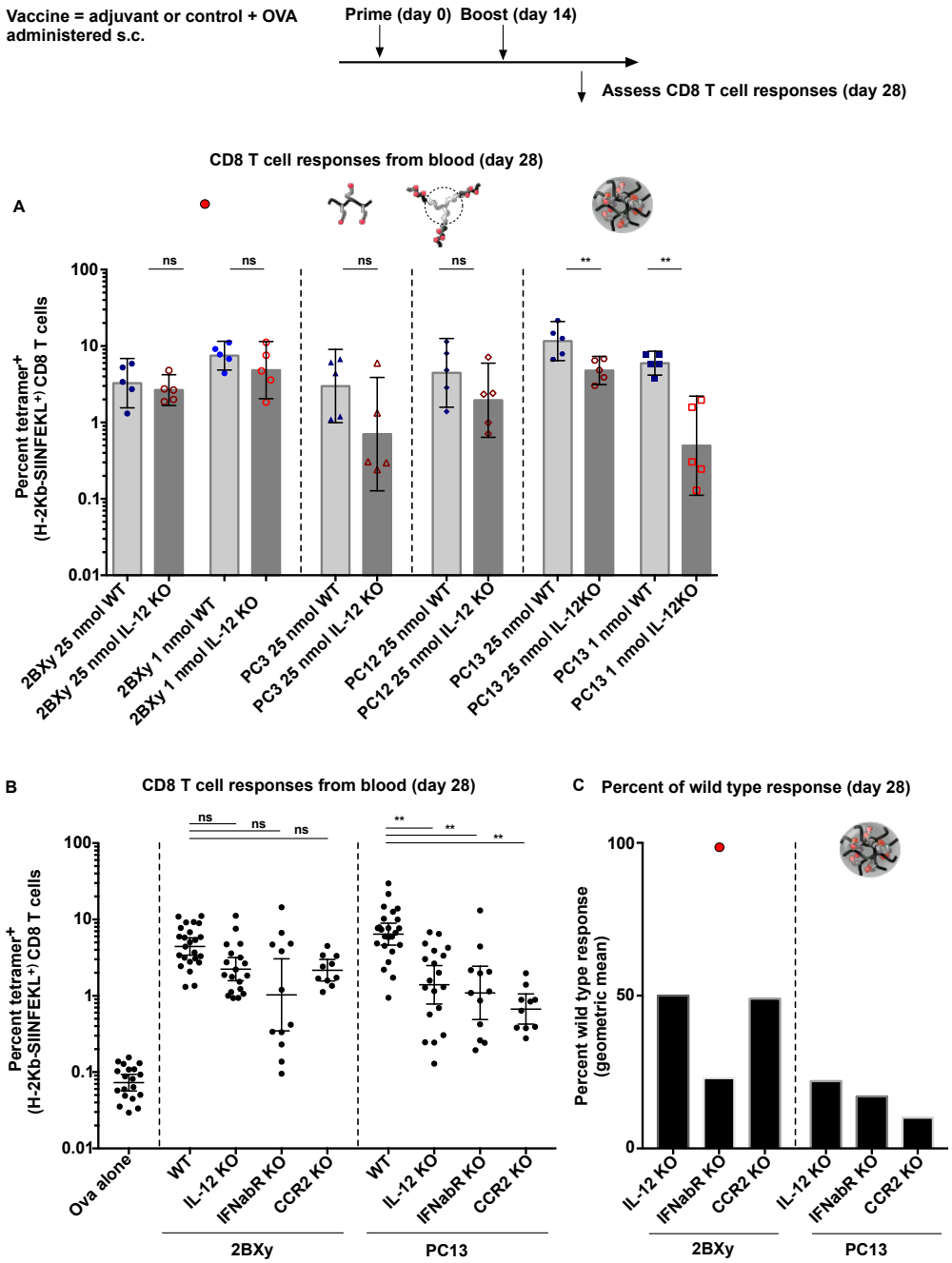

Figure 6. CD8 T cell responses by the submicron particle polymer-TLR-7/8a conjugate, but not the small molecule TLR-7/8a, 2BXy, depend on monocytes and IL-12. (A-C) Different TLR-7/8a compositions normalized for dose (25 or 1 nmol) were admixed with 50 μg of OVA in PBS and given subcutaneously to either wild type, IL-12 deficient (IL-12 KO), CCR2 deficient (CCR2 KO) or IFNαβR deficient (IFNαβR KO) mice at days 0 and 14. (A) Antigen-specific CD8 T cell responses were evaluated from whole blood of WT or IL-12 KO mice at day 28. (B) Day 28 CD8 T cell responses evaluated from blood of WT, IL-12 KO, CCR2 KO and IFNαβR KO mice (n = 10-25) compiled from three independent studies. (C) Responses in knockout mice are represented as the percent observed in wild type mice from panel (B). Data are reported as geometric mean with 95% CI. Comparison of multiple groups for statistical significance was determined using one-way ANOVA with Bonferroni correction; comparison of two groups for statistical significance in panel (A) was determined using a student's t-test; ns = not significant; *, p = 0.05; **, p = 0.01. PP = polymer precursor; PC = polymer conjugate.

DISCUSSION

The ability of agonists of TLR-3, TLR-7/8, TLR-9 and STING to induce CD8 T cell immunity when combined with protein or peptide antigens requires the use of formulations that restrict and prolong adjuvant activity within lymphoid tissue [21, 23, 28, 42, 73, 74]. While covalent attachment (conjugation) of TLRa to macromolecular carriers has emerged as an effective strategy for modulating the PK of TLRa to enhance CD8 T cell

immunity, it is presently not well understood how various parameters of macromolecular TLRa conjugates impact innate and adaptive immunity *in vivo*. Therefore, a major goal of this study was to determine how attachment of TLR-7/8a to polymers with different composition, chain architecture and hydrodynamic behavior impacts the efficiency and mechanism of CD8 T cell induction *in vivo*.

Among the polymer-TLR-7/8a conjugates evaluated herein, we observed a trend between increasing hydrodynamic radius and increased magnitude of both lymph node IL-12 production and antigen-specific CD8 T cells induced following vaccination. Accordingly, polymer-TLR-7/8a conjugates that form submicron particles (R_H ~ 300 nm) led to the highest magnitude lymph node IL-12 and CD8 T cell responses, followed by polymer micelles (~10 nm) and then random coil polymers (~ 4 nm). Our observation that the submicron particle is phagocytized more efficiently by both migratory and lymph node resident APCs as compared with the micelle and random coil polymers provides a possible mechanism to account for the observed differences in adjuvant activity between the different polymer-TLR-7/8a conjugate compositions. Indeed, flexible

random coil polymers based on PEG and HPMA have been specifically selected for drug delivery applications based on their ability to evade capture by phagocytic cells [75-77]. Though limited APC capture by random coil polymers is likely dependent on a number of factors, including polymer charge [78], this characteristic may ultimately limit their utility as carriers of certain TLRa, such as TLR-7/8a, and other drug molecules that require APC uptake to access intracellularly localized receptors. An additional notable finding was that, while polymers alone can have intrinsic adjuvant properties depending on molecular weight and composition [79-81], none of the HPMA-based polymer precursors (*i.e.* polymer alone without TLR-7/8a attached) induced a significant increase in lymph node cytokines or CD8 T cells as compared with untreated animals, which is consistent with prior reports that HPMA polymers are immunologically inert carriers [54, 55].

As prior studies by others and us have found that water-soluble, small molecule TLR-7/8a (*e.g.*, R848), when not properly formulated, are poor adjuvants for vaccines [21, 41, 82], it was perhaps unexpected that the unformulated TLR-7/8a, 2BXy, induced robust CD8

T cell responses. While 2BXy has higher *in vitro* potency than R848, this alone likely does not account for the markedly different adjuvant activity of these two molecules. Indeed, one possible explanation is that the addition of the xylene linker makes 2BXy more lipophilic than R848 and that this leads to greater tissue retention than R848. This dependence of lipophilic characteristics on injection site localization was previously observed with benzonaphthyridine-based TLR-7a by Wu *et al*[41]. Consistent with this hypothesis, we observed that 2BXy had a slower rate of clearance from all tissues, including DLN, as compared with R848. Slower clearance resulted in 2BXy sustaining concentrations exceeding EC50 (threshold for activity) in vaccine-site DLN for several days, which was temporally associated with lymph node cytokine production and lymph node swelling. In contrast, R848 induced no lymph node cytokines, possibly because concentrations of R848 never exceeded EC50 in DLN. Another important finding was that while 2BXy concentrations in spleen exceeded EC50 for up to 5 days, cytokines were only measurable in blood (systemically) for up to 24 hours. These data suggest that splenic immune activation can be achieved independently of systemic (*i.e.* blood) inflammation that is associated with vaccine/adjuvant toxicity [65], which indicates that it

may be possible to target vaccines to the spleen [2, 83] with minimal inflammation spillover to the blood.

Prior studies have reported that virus-sized (~ 20-200 nm) particles are optimal for inducing T cell immunity based on their ability to passively traffic to lymph nodes and target uptake by lymph node resident dendritic cells [24, 44, 45, 84]. Therefore, the data reported herein showing that TLR-7/8a compositions with extremes of size, a small molecule (< 1 nm) and a submicron particle (~ 300 nm), induced comparable, high magnitude CD8 T cell immunity was unexpected. While CD8 T cell responses by the submicron particle were dependent on CCR2+ monocyte recruitment and IL-12 production, CD8 T cell responses by the small molecule showed less dependence on monocytes and IL-12 but a requirement for Type I IFNs. A possible mechanism to account for these findings is that the small molecule disperses rapidly from the injection site and passively reaches lymph node resident DCs that produce Type I IFNs, while the submicron particle is retained at the injection site and is engulfed by migratory monocytes that traffic to lymph nodes and preferentially produce IL-12. Alternatively,

and not mutually exclusive, the different formulations of TLR-7/8a could result in differences in intracellular compartmentalization within the same APC subsets and thereby signal through different pathways that result in distinct patterns of cytokine production, which has been observed for different formulations of CpG (TLR-9a) [85, 86]. The finding that different formulations of the same innate immune stimulus (*i.e.* TLR-7/8a) can induce CD8 T cell immunity with a varying degree of dependence on monocytes may have important implications for the design of vaccines seeking to avoid or leverage such a role of monocytes. While additional studies will be needed to dissect the exact mechanism of monocyte involvement in the generation of CD8 T cell immunity and how monocytes imprint on the quality of the adaptive immune response, our results add to a growing body of literature showing that monocytes can function in the promotion of T cell immunity [68-71, 87, 88]. Accordingly, De Koker *et al* recently showed that both CD4 and CD8 T cell immunity induced by a protein vaccine combined with a TLR-9a (CpG) was dependent on monocytes, which were identified as the primary source of the critical Th1-skewing cytokine, IL-12 [70]. In addition to supporting T cell immunity

through cytokine production, monocytes have recently been shown to present antigen to CD4 T cells and even cross-present antigen to CD8 T cells, a function previously thought to be exclusive to BATF3+ DCs [68]. The ability of monocytes to present antigen appears to be highly dependent on the nature of the innate immune stimulus, as Jakubzick *et al* found that monocytes cross-present antigen when stimulated with agonists of TLR-7 but not agonists of TLR-3 (pI:C), TLR-4 (LPS) or TLR-9 (CpG) [69].

CONCLUSIONS

The data presented shows how different properties of small molecule TLR-7/8a and polymer-TLR-7/8a conjugates impact the location, magnitude and duration of innate immune activity as well as how such parameters impact the potency and mechanism of TLR-7/8a as adjuvants for inducing CD8 T cell immunity. Such results may aid the rationale design of adjuvants for precisely modulating the type, amount and location of inflammation desired for a specific application. For example, our results show that the partitioning of adjuvant from systemic circulation to lymphoid tissues can be achieved on the basis of adjuvant size; that the magnitude of lymph node cytokines and CD8 T

cell responses can be altered through the modulation of carrier architecture; and that different formulations of the same innate stimulus can be used to promote CD8 T cell immunity through distinct immunological mechanisms. Overall, this study will help inform the development of safer and more effective vaccines for inducing CD8 T cell immunity and, more generally, will contribute to a deeper understanding of the complex interplay between materials and the immune system.

ASSOCIATED CONTENT

Supporting Information

Reaction schemes depicting synthetic routes for the preparation of the polymer-TLR-7/8a conjugates. Tables showing physicochemical characteristics of the polymer precursors and polymer-TLR-7/8a conjugates; and pharmacokinetic parameters for unformulated 2BXy and R848 adjuvants. Figures showing *in vitro* dose response curves of the unformulated TLR-7/8a; the hydrodynamic properties of polymer-TLR-7/8a conjugates; the impact of TLR-7/8a density on the capacity of the polymer-TLR-7/8a conjugates to induce cytokine production *in vitro*; the *in vivo* assessment of the

biological activity of non-targeted and mannose-targeted polymer-TLR-7/8a conjugates; chromatography experiments used to evaluate interactions between the protein antigen (Ovalbumin) and polymer conjugates; and, the kinetics of blood cytokines induced by the unformulated TLR-7/8a. The following file is available free of charge:

Laga_supplementary data_Biomacromolecules.pdf

AUTHOR INFORMATION

Corresponding Author

* Phone: +420-325 873 806. Fax: +420-296 809 410. Email: laga@imc.cas.cz

Author Contributions

The manuscript was written through contributions of all authors. All authors have given approval to the final version of the manuscript. ‡These authors contributed equally.

ACKNOWLEDGMENT

The authors acknowledge Marlon Dillon, Gloria Salbador, and Carmelo Chiedi for expert veterinary technical assistance. This work was supported by the Intramural Research

Program of the U.S. National Institutes of Health, the Czech Science Foundation (project 16-14957Y) and the Ministry of Education, Youth and Sports of the Czech Republic within the National Sustainability Program II (project BIOCEV-FAR LQ1604).

REFERENCES

1. Plotkin, S. A., Correlates of protection induced by vaccination. *Clinical and vaccine immunology : CVI* **2010,** 17, (7), 1055-65.

2. Ishizuka, A. S.; Lyke, K. E.; DeZure, A.; Berry, A. A.; Richie, T. L.; Mendoza, F. H.; Enama, M. E.; Gordon, I. J.; Chang, L. J.; Sarwar, U. N.; Zephir, K. L.; Holman, L. A.; James, E. R.; Billingsley, P. F.; Gunasekera, A.; Chakravarty, S.; Manoj, A.; Li, M.; Ruben, A. J.; Li, T.; Eappen, A. G.; Stafford, R. E.; K, C. N.; Murshedkar, T.; DeCederfelt, H.; Plummer, S. H.; Hendel, C. S.; Novik, L.; Costner, P. J.; Saunders, J. G.; Laurens, M. B.; Plowe, C. V.; Flynn, B.; Whalen, W. R.; Todd, J. P.; Noor, J.; Rao, S.; Sierra-Davidson, K.; Lynn, G. M.; Epstein, J. E.; Kemp, M. A.; Fahle, G. A.; Mikolajczak, S. A.; Fishbaugher, M.; Sack, B. K.; Kappe, S. H.; Davidson, S. A.; Garver, L. S.; Bjorkstrom, N. K.; Nason, M. C.; Graham, B. S.; Roederer, M.; Sim, B. K.; Hoffman, S. L.; Ledgerwood, J. E.; Seder, R. A., Protection against malaria at 1 year and immune correlates following PfSPZ vaccination. *Nature medicine* **2016**, 22 (6), 614-623.

3. Sullivan, N. J.; Hensley, L.; Asiedu, C.; Geisbert, T. W.; Stanley, D.; Johnson, J.; Honko, A.; Olinger, G.; Bailey, M.; Geisbert, J. B.; Reimann, K. A.; Bao, S.; Rao, S.; Roederer, M.; Jahrling, P. B.; Koup, R. A.; Nabel, G. J., CD8+ cellular immunity mediates rAd5 vaccine protection against Ebola virus infection of nonhuman primates. *Nature medicine* **2011,** 17, (9), 1128-31.

4. Chen, D. S.; Mellman, I., Oncology meets immunology: the cancer-immunity cycle. *Immunity* **2013,** 39, (1), 1-10.

5. Schlom, J., Therapeutic cancer vaccines: current status and moving forward. *Journal of the National Cancer Institute* **2012,** 104, (8), 599-613.

6. Kenter, G. G.; Welters, M. J.; Valentijn, A. R.; Lowik, M. J.; Berends-van der Meer, D. M.; Vloon, A. P.; Essahsah, F.; Fathers, L. M.; Offringa, R.; Drijfhout, J. W.; Wafelman, A. R.; Oostendorp, J.; Fleuren, G. J.; van der Burg, S. H.; Melief, C. J., Vaccination against HPV-16 oncoproteins for vulvar intraepithelial neoplasia. *N Engl J Med* **2009,** 361, (19), 1838-47.

7. Brito, L. A.; O'Hagan, D. T., Designing and building the next generation of improved vaccine adjuvants. *Journal of controlled release : official journal of the Controlled Release Society* **2014,** 190C, 563-579.

8. Iwasaki, A.; Medzhitov, R., Toll-like receptor control of the adaptive immune responses. *Nat Immunol* **2004,** 5, (10), 987-95.

9. Diebold, S. S.; Kaisho, T.; Hemmi, H.; Akira, S.; Reis e Sousa, C., Innate antiviral responses by means of TLR7-mediated recognition of single-stranded RNA. *Science* **2004,** 303, (5663), 1529-31.

10. Coffman, R. L.; Sher, A.; Seder, R. A., Vaccine adjuvants: putting innate immunity to work. *Immunity* **2010,** 33, (4), 492-503.

11. Gorden, K. B.; Gorski, K. S.; Gibson, S. J.; Kedl, R. M.; Kieper, W. C.; Qiu, X. H.; Tomai, M. A.; Alkan, S. S.; Vasilakos, J. P., Synthetic TLR Agonists reveal functional differences between human TLR7 and TLR8. *Journal of Immunology* **2005,** 174, (3), 1259-1268.

12. Kurimoto, A.; Ogino, T.; Ichii, S.; Isobe, Y.; Tobe, M.; Ogita, H.; Takaku, H.; Sajiki, H.; Hirota, K.; Kawakami, H., Synthesis and evaluation of 2-substituted 8-hydroxyadenines as potent interferon inducers with improved oral bioavailabilities. *Bioorg Med Chem* **2004,** 12, (5), 1091-9.

13. Gerster, J. F.; Lindstrom, K. J.; Miller, R. L.; Tomai, M. A.; Birmachu, W.; Bomersine, S. N.; Gibson, S. J.; Imbertson, L. M.; Jacobson, J. R.; Knafla, R. T.; Maye, P. V.; Nikolaides, N.; Oneyemi, F. Y.; Parkhurst, G. J.; Pecore, S. E.; Reiter, M. J.; Scribner, L. S.; Testerman, T. L.; Thompson, N. J.; Wagner, T. L.; Weeks, C. E.; Andre, J. D.; Lagain, D.; Bastard, Y.; Lupu, M., Synthesis and structure-activity-relationships of

1H-imidazo[4,5-c]quinolines that induce interferon production. *J Med Chem* **2005,** 48, (10), 3481-91.

14. Czarniecki, M., Small molecule modulators of toll-like receptors. *Journal of medicinal chemistry* **2008,** 51, (21), 6621-6.

15. Shukla, N. M.; Malladi, S. S.; Mutz, C. A.; Balakrishna, R.; David, S. A., Structure-activity relationships in human toll-like receptor 7-active imidazoquinoline analogues. *J Med Chem* **2010,** 53, (11), 4450-65.

16. A, A. G.; Tyring, S. K.; Rosen, T., Beyond a decade of 5% imiquimod topical therapy. *Journal of drugs in dermatology : JDD* **2009,** 8, (5), 467-74.

17. Gunzer, M.; Riemann, H.; Basoglu, Y.; Hillmer, A.; Weishaupt, C.; Balkow, S.; Benninghoff, B.; Ernst, B.; Steinert, M.; Scholzen, T.; Sunderkotter, C.; Grabbe, S., Systemic administration of a TLR7 ligand leads to transient immune incompetence due to peripheral-blood leukocyte depletion. *Blood* **2005,** 106, (7), 2424-32.

18. Soria, I.; Myhre, P.; Horton, V.; Ellefson, P.; McCarville, S.; Schmitt, K.; Owens, M., Effect of food on the pharmacokinetics and bioavailability of oral imiquimod relative to a subcutaneous dose. *International journal of clinical pharmacology and therapeutics* **2000,** 38, (10), 476-81.

19. Dudek, A. Z.; Yunis, C.; Harrison, L. I.; Kumar, S.; Hawkinson, R.; Cooley, S.; Vasilakos, J. P.; Gorski, K. S.; Miller, J. S., First in human phase I trial of 852A, a novel systemic toll-like receptor 7 agonist, to activate innate immune responses in patients with advanced cancer. *Clin Cancer Res* **2007,** 13, (23), 7119-25.

20. Harrison, L. I.; Astry, C.; Kumar, S.; Yunis, C., Pharmacokinetics of 852A, an imidazoquinoline Toll-like receptor 7-specific agonist, following intravenous, subcutaneous, and oral administrations in humans. *Journal of clinical pharmacology* **2007,** 47, (8), 962-9.

21. Lynn, G. M.; Laga, R.; Darrah, P. A.; Ishizuka, A. S.; Balaci, A. J.; Dulcey, A. E.; Pechar, M.; Pola, R.; Gerner, M. Y.; Yamamoto, A.; Buechler, C. R.; Quinn, K. M.; Smelkinson, M. G.; Vanek, O.; Cawood, R.; Hills, T.; Vasalatiy, O.; Kastenmuller, K.; Francica, J. R.; Stutts, L.; Tom, J. K.; Ryu, K. A.; Esser-Kahn, A. P.; Etrych, T.; Fisher, K. D.; Seymour, L. W.; Seder, R. A., In vivo characterization of the physicochemical

properties of polymer-linked TLR agonists that enhance vaccine immunogenicity. *Nat Biotechnol* **2015,** 33, (11), 1201-10.

22. Oh, J. Z.; Kedl, R. M., The capacity to induce cross-presentation dictates the success of a TLR7 agonist-conjugate vaccine for eliciting cellular immunity. *J Immunol* **2010,** 185, (8), 4602-8.

23. Kastenmuller, K.; Wille-Reece, U.; Lindsay, R. W.; Trager, L. R.; Darrah, P. A.; Flynn, B. J.; Becker, M. R.; Udey, M. C.; Clausen, B. E.; Igyarto, B. Z.; Kaplan, D. H.; Kastenmuller, W.; Germain, R. N.; Seder, R. A., Protective T cell immunity in mice following protein-TLR7/8 agonist-conjugate immunization requires aggregation, type I IFN, and multiple DC subsets. *J Clin Invest* **2011,** 121, (5), 1782-96.

24. Bachmann, M. F.; Jennings, G. T., Vaccine delivery: a matter of size, geometry, kinetics and molecular patterns. *Nat Rev Immunol* **2010,** 10, (11), 787-96.

25. Kasturi, S. P.; Skountzou, I.; Albrecht, R. A.; Koutsonanos, D.; Hua, T.; Nakaya, H. I.; Ravindran, R.; Stewart, S.; Alam, M.; Kwissa, M.; Villinger, F.; Murthy, N.; Steel, J.; Jacob, J.; Hogan, R. J.; Garcia-Sastre, A.; Compans, R.; Pulendran, B., Programming the magnitude and persistence of antibody responses with innate immunity. *Nature* **2011,** 470, (7335), 543-7.

26. Tacken, P. J.; Zeelenberg, I. S.; Cruz, L. J.; van Hout-Kuijer, M. A.; van de Glind, G.; Fokkink, R. G.; Lambeck, A. J.; Figdor, C. G., Targeted delivery of TLR ligands to human and mouse dendritic cells strongly enhances adjuvanticity. *Blood* **2011,** 118, (26), 6836-44.

27. Ilyinskii, P. O.; Roy, C. J.; O'Neil, C. P.; Browning, E. A.; Pittet, L. A.; Altreuter, D. H.; Alexis, F.; Tonti, E.; Shi, J.; Basto, P. A.; Iannacone, M.; Radovic-Moreno, A. F.; Langer, R. S.; Farokhzad, O. C.; von Andrian, U. H.; Johnston, L. P.; Kishimoto, T. K., Adjuvant-carrying synthetic vaccine particles augment the immune response to encapsulated antigen and exhibit strong local immune activation without inducing systemic cytokine release. *Vaccine* **2014,** 32, (24), 2882-95.

28. Smirnov, D.; Schmidt, J. J.; Capecchi, J. T.; Wightman, P. D., Vaccine adjuvant activity of 3M-052: an imidazoquinoline designed for local activity without systemic cytokine induction. *Vaccine* **2011,** 29, (33), 5434-42.

29. Van Hoeven, N.; Fox, C. B.; Granger, B.; Evers, T.; Joshi, S. W.; Nana, G. I.; Evans, S. C.; Lin, S.; Liang, H.; Liang, L.; Nakajima, R.; Felgner, P. L.; Bowen, R. A.; Marlenee, N.; Hartwig, A.; Baldwin, S. L.; Coler, R. N.; Tomai, M.; Elvecrog, J.; Reed, S. G.; Carter, D., A Formulated TLR7/8 Agonist is a Flexible, Highly Potent and Effective Adjuvant for Pandemic Influenza Vaccines. *Sci Rep* **2017,** 7, 46426.

30. Scott, E. A.; Stano, A.; Gillard, M.; Maio-Liu, A. C.; Swartz, M. A.; Hubbell, J. A., Dendritic cell activation and T cell priming with adjuvant- and antigen-loaded oxidation-sensitive polymersomes. *Biomaterials* **2012,** 33, (26), 6211-9.

31. Sevimli, S.; Knight, F. C.; Gilchuk, P.; Joyce, S.; Wilson, J. T., Fatty Acid-Mimetic Micelles for Dual Delivery of Antigens and Imidazoquinoline Adjuvants. *ACS Biomaterials Science & Engineering* **2017,** 3, (2), 179-194.

32. Rodell, C. B.; Arlauckas, S. P.; Cuccarese, M. F.; Garris, C. S.; Li, R.; Ahmed, M. S.; Kohler, R. H.; Pittet, M. J.; Weissleder, R., TLR7/8-agonist-loaded nanoparticles promote the polarization of tumour-associated macrophages to enhance cancer immunotherapy. *Nature Biomedical Engineering* **2018,** 2, (8), 578-588.

33. Ignacio, B. J.; Albin, T. J.; Esser-Kahn, A. P.; Verdoes, M., Toll-like Receptor Agonist Conjugation: A Chemical Perspective. *Bioconjug Chem* **2018,** 29, (3), 587-603.

34. Shukla, N. M.; Lewis, T. C.; Day, T. P.; Mutz, C. A.; Ukani, R.; Hamilton, C. D.; Balakrishna, R.; David, S. A., Toward self-adjuvanting subunit vaccines: model peptide and protein antigens incorporating covalently bound toll-like receptor-7 agonistic imidazoquinolines. *Bioorg Med Chem Lett* **2011,** 21, (11), 3232-6.

35. Vecchi, S.; Bufali, S.; Uno, T.; Wu, T.; Arcidiacono, L.; Filippini, S.; Rigat, F.; O'Hagan, D., Conjugation of a TLR7 agonist and antigen enhances protection in the S. pneumoniae murine infection model. *European journal of pharmaceutics and biopharmaceutics : official journal of Arbeitsgemeinschaft fur Pharmazeutische Verfahrenstechnik e.V* **2014,** 87, (2), 310-7.

36. Shukla, N. M.; Salunke, D. B.; Balakrishna, R.; Mutz, C. A.; Malladi, S. S.; David, S. A., Potent adjuvanticity of a pure TLR7-agonistic imidazoquinoline dendrimer. *PLoS One* **2012,** 7, (8), e43612.

37. Yoo, E.; Salyer, A. C. D.; Brush, M. J. H.; Li, Y.; Trautman, K. L.; Shukla, N. M.; De Beuckelaer, A.; Lienenklaus, S.; Deswarte, K.; Lambrecht, B. N.; De Geest, B. G.;

David, S. A., Hyaluronic Acid Conjugates of TLR7/8 Agonists for Targeted Delivery to Secondary Lymphoid Tissue. *Bioconjug Chem* **2018,** 29, (8), 2741-2754.

38. Francica, J. R.; Lynn, G. M.; Laga, R.; Joyce, M. G.; Ruckwardt, T. J.; Morabito, K. M.; Chen, M.; Chaudhuri, R.; Zhang, B.; Sastry, M.; Druz, A.; Ko, K.; Choe, M.; Pechar, M.; Georgiev, I. S.; Kueltzo, L. A.; Seymour, L. W.; Mascola, J. R.; Kwong, P. D.; Graham, B. S.; Seder, R. A., Thermoresponsive Polymer Nanoparticles Co-deliver RSV F Trimers with a TLR-7/8 Adjuvant. *Bioconjugate Chem* **2016,** 27, (10), 2372-2385.

39. Nuhn, L.; Vanparijs, N.; De Beuckelaer, A.; Lybaert, L.; Verstraete, G.; Deswarte, K.; Lienenklaus, S.; Shukla, N. M.; Salyer, A. C.; Lambrecht, B. N.; Grooten, J.; David, S. A.; De Koker, S.; De Geest, B. G., pH-degradable imidazoquinoline-ligated nanogels for lymph node-focused immune activation. *Proc Natl Acad Sci U S A* **2016,** 113, (29), 8098-103.

40. Nuhn, L.; Van Hoecke, L.; Deswarte, K.; Schepens, B.; Li, Y.; Lambrecht, B. N.; De Koker, S.; David, S. A.; Saelens, X.; De Geest, B. G., Potent anti-viral vaccine adjuvant based on pH-degradable nanogels with covalently linked small molecule imidazoquinoline TLR7/8 agonist. *Biomaterials* **2018,** 178, 643-651.

41. Wu, T. Y.; Singh, M.; Miller, A. T.; De Gregorio, E.; Doro, F.; D'Oro, U.; Skibinski, D. A.; Mbow, M. L.; Bufali, S.; Herman, A. E.; Cortez, A.; Li, Y.; Nayak, B. P.; Tritto, E.; Filippi, C. M.; Otten, G. R.; Brito, L. A.; Monaci, E.; Li, C.; Aprea, S.; Valentini, S.; Calabromicron, S.; Laera, D.; Brunelli, B.; Caproni, E.; Malyala, P.; Panchal, R. G.; Warren, T. K.; Bavari, S.; O'Hagan, D. T.; Cooke, M. P.; Valiante, N. M., Rational design of small molecules as vaccine adjuvants. *Sci Transl Med* **2014,** 6, (263), 263ra160.

42. Liu, H.; Moynihan, K. D.; Zheng, Y.; Szeto, G. L.; Li, A. V.; Huang, B.; Van Egeren, D. S.; Park, C.; Irvine, D. J., Structure-based programming of lymph-node targeting in molecular vaccines. *Nature* **2014,** 507, (7493), 519-22.

43. Ravkov, E. V.; Williams, M. A., The magnitude of CD4+ T cell recall responses is controlled by the duration of the secondary stimulus. *J Immunol* **2009,** 183, (4), 2382-9.

44. Manolova, V.; Flace, A.; Bauer, M.; Schwarz, K.; Saudan, P.; Bachmann, M. F., Nanoparticles target distinct dendritic cell populations according to their size. *Eur J Immunol* **2008,** 38, (5), 1404-13.

45. Reddy, S. T.; Rehor, A.; Schmoekel, H. G.; Hubbell, J. A.; Swartz, M. A., In vivo targeting of dendritic cells in lymph nodes with poly(propylene sulfide) nanoparticles. *Journal of controlled release : official journal of the Controlled Release Society* **2006,** 112, (1), 26-34.

46. Gerner, M. Y.; Torabi-Parizi, P.; Germain, R. N., Strategically localized dendritic cells promote rapid T cell responses to lymph-borne particulate antigens. *Immunity* **2015,** 42, (1), 172-85.

47. Li, A. V.; Moon, J. J.; Abraham, W.; Suh, H.; Elkhader, J.; Seidman, M. A.; Yen, M.; Im, E. J.; Foley, M. H.; Barouch, D. H.; Irvine, D. J., Generation of effector memory T cell-based mucosal and systemic immunity with pulmonary nanoparticle vaccination. *Sci Transl Med* **2013,** 5, (204), 204ra130.

48. Shukla, N. M.; Mutz, C. A.; Ukani, R.; Warshakoon, H. J.; Moore, D. S.; David, S. A., Syntheses of fluorescent imidazoquinoline conjugates as probes of Toll-like receptor 7. *Bioorg Med Chem Lett* **2010,** 20, (22), 6384-6.

49. Ulbrich, K.; Subr, V.; Strohalm, J.; Plocova, D.; Jelinkova, M.; Rihova, B., Polymeric drugs based on conjugates of synthetic and natural macromolecules. I. Synthesis and physico-chemical characterisation. *Journal of controlled release : official journal of the Controlled Release Society* **2000,** 64, (1-3), 63-79.

50. Reschel, T.; Konak, C.; Oupicky, D.; Seymour, L. W.; Ulbrich, K., Physical properties and in vitro transfection efficiency of gene delivery vectors based on complexes of DNA with synthetic polycations. *Journal of Controlled Release* **2002,** 81, (1-2), 201-217.

51. Ulbrich, K.; Subr, V., Structural and chemical aspects of HPMA copolymers as drug carriers. *Advanced drug delivery reviews* **2010,** 62, (2), 150-66.

52. Pearce, O. M. T.; Fisher, K. D.; Humphries, J.; Seymour, L. W.; Smith, A.; Davis, B. G., Glycoviruses: Chemical glycosylation retargets adenoviral gene transfer. *Angew Chem Int Edit* **2005,** 44, (7), 1057-1061.

53. Seymour, L. W.; Ferry, D. R.; Anderson, D.; Hesslewood, S.; Julyan, P. J.; Poyner, R.; Doran, J.; Young, A. M.; Burtles, S.; Kerr, D. J.; Cancer Research Campaign Phase, I. I. I. C. T. c., Hepatic drug targeting: phase I evaluation of polymer-bound doxorubicin. *J Clin Oncol* **2002,** 20, (6), 1668-76.

54. Duncan, R.; Vicent, M. J., Do HPMA copolymer conjugates have a future as clinically useful nanomedicines? A critical overview of current status and future opportunities. *Advanced drug delivery reviews* **2010,** 62, (2), 272-82.

55. Liu, X. M.; Miller, S. C.; Wang, D., Beyond oncology--application of HPMA copolymers in non-cancerous diseases. *Advanced drug delivery reviews* **2010,** 62, (2), 258-71.

56. Seymour, L. W.; Duncan, R.; Strohalm, J.; Kopecek, J., Effect of Molecular-Weight (Mbarw) of N-(2-Hydroxypropyl)Methacrylamide Copolymers on Body Distribution and Rate of Excretion after Subcutaneous, Intraperitoneal, and Intravenous Administration to Rats. *J Biomed Mater Res* **1987,** 21, (11), 1341-1358.

57. Chiefari, J.; Chong, Y. K.; Ercole, F.; Krstina, J.; Jeffery, J.; Le, T. P. T.; Mayadunne, R. T. A.; Meijs, G. F.; Moad, C. L.; Moad, G.; Rizzardo, E.; Thang, S. H., Living Free-Radical Polymerization by Reversible Addition,àíFragmentation Chain Transfer:,Äâ The RAFT Process. *Macromolecules* **1998,** 31, (16), 5559-5562.

58. Chytil, P.; Etrych, T.; Kriz, J.; Subr, V.; Ulbrich, K., N-(2-Hydroxypropyl)methacrylamide-based polymer conjugates with pH-controlled activation of doxorubicin for cell-specific or passive tumour targeting. Synthesis by RAFT polymerisation and physicochemical characterisation. *European journal of pharmaceutical sciences : official journal of the European Federation for Pharmaceutical Sciences* **2010,** 41, (3-4), 473-82.

59. Pola, R.; Braunova, A.; Laga, R.; Pechar, M.; Ulbrich, K., Click chemistry as a powerful and chemoselective tool for the attachment of targeting ligands to polymer drug carriers. *Polymer Chemistry* **2014,** 5, (4), 1340-1350.

60. De Coen, R.; Vanparijs, N.; Risseeuw, M. D.; Lybaert, L.; Louage, B.; De Koker, S.; Kumar, V.; Grooten, J.; Taylor, L.; Ayres, N.; Van Calenbergh, S.; Nuhn, L.; De Geest, B. G., pH-Degradable Mannosylated Nanogels for Dendritic Cell Targeting. *Biomacromolecules* **2016,** 17, (7), 2479-88.

61. Cui, L.; Cohen, J. A.; Broaders, K. E.; Beaudette, T. T.; Frechet, J. M., Mannosylated dextran nanoparticles: a pH-sensitive system engineered for immunomodulation through mannose targeting. *Bioconjug Chem* **2011,** 22, (5), 949-57.

62. Ribeiro-Viana, R.; Sanchez-Navarro, M.; Luczkowiak, J.; Koeppe, J. R.; Delgado, R.; Rojo, J.; Davis, B. G., Virus-like glycodendrinanoparticles displaying quasi-equivalent nested polyvalency upon glycoprotein platforms potently block viral infection. *Nat Commun* **2012,** 3, 1303.

63. Unger, W. W.; van Beelen, A. J.; Bruijns, S. C.; Joshi, M.; Fehres, C. M.; van Bloois, L.; Verstege, M. I.; Ambrosini, M.; Kalay, H.; Nazmi, K.; Bolscher, J. G.; Hooijberg, E.; de Gruijl, T. D.; Storm, G.; van Kooyk, Y., Glycan-modified liposomes boost CD4+ and CD8+ T-cell responses by targeting DC-SIGN on dendritic cells. *Journal of controlled release : official journal of the Controlled Release Society* **2012,** 160, (1), 88-95.

64. Fehres, C. M.; Kalay, H.; Bruijns, S. C.; Musaafir, S. A.; Ambrosini, M.; van Bloois, L.; van Vliet, S. J.; Storm, G.; Garcia-Vallejo, J. J.; van Kooyk, Y., Cross-presentation through langerin and DC-SIGN targeting requires different formulations of glycan-modified antigens. *Journal of controlled release : official journal of the Controlled Release Society* **2015,** 203, 67-76.

65. Cristofaro, P.; Opal, S. M., The Toll-like receptors and their role in septic shock. *Expert opinion on therapeutic targets* **2003,** 7, (5), 603-12.

66. Padovan, E.; Spagnoli, G. C.; Ferrantini, M.; Heberer, M., IFN-alpha2a induces IP-10/CXCL10 and MIG/CXCL9 production in monocyte-derived dendritic cells and enhances their capacity to attract and stimulate CD8+ effector T cells. *Journal of leukocyte biology* **2002,** 71, (4), 669-76.

67. Keppler, S. J.; Rosenits, K.; Koegl, T.; Vucikuja, S.; Aichele, P., Signal 3 cytokines as modulators of primary immune responses during infections: the interplay of type I IFN and IL-12 in CD8 T cell responses. *PLoS One* **2012,** 7, (7), e40865.

68. Jakubzick, C. V.; Randolph, G. J.; Henson, P. M., Monocyte differentiation and antigen-presenting functions. *Nat Rev Immunol* **2017,** 17, (6), 349-362.

69. Larson, S. R.; Atif, S. M.; Gibbings, S. L.; Thomas, S. M.; Prabagar, M. G.; Danhorn, T.; Leach, S. M.; Henson, P. M.; Jakubzick, C. V., Ly6C(+) monocyte efferocytosis and cross-presentation of cell-associated antigens. *Cell Death Differ* **2016,** 23, (6), 997-1003.

70. De Koker, S.; Van Hoecke, L.; De Beuckelaer, A.; Roose, K.; Deswarte, K.; Willart, M. A.; Bogaert, P.; Naessens, T.; De Geest, B. G.; Saelens, X.; Lambrecht, B. N.; Grooten, J., Inflammatory monocytes regulate Th1 oriented immunity to CpG adjuvanted protein vaccines through production of IL-12. *Sci Rep* **2017,** 7, (1), 5986.

71. Nakano, H.; Lin, K. L.; Yanagita, M.; Charbonneau, C.; Cook, D. N.; Kakiuchi, T.; Gunn, M. D., Blood-derived inflammatory dendritic cells in lymph nodes stimulate acute T helper type 1 immune responses. *Nat Immunol* **2009,** 10, (4), 394-402.

72. Le Bon, A.; Durand, V.; Kamphuis, E.; Thompson, C.; Bulfone-Paus, S.; Rossmann, C.; Kalinke, U.; Tough, D. F., Direct stimulation of T cells by type I IFN enhances the CD8+ T cell response during cross-priming. *J Immunol* **2006,** 176, (8), 4682-9.

73. Hanson, M. C.; Crespo, M. P.; Abraham, W.; Moynihan, K. D.; Szeto, G. L.; Chen, S. H.; Melo, M. B.; Mueller, S.; Irvine, D. J., Nanoparticulate STING agonists are potent lymph node-targeted vaccine adjuvants. *J Clin Invest* **2015,** 125, (6), 2532-46.

74. Jewell, C. M.; Lopez, S. C.; Irvine, D. J., In situ engineering of the lymph node microenvironment via intranodal injection of adjuvant-releasing polymer particles. *Proc Natl Acad Sci U S A* **2011,** 108, (38), 15745-50.

75. Mori, A.; Klibanov, A. L.; Torchilin, V. P.; Huang, L., Influence of the steric barrier activity of amphipathic poly(ethyleneglycol) and ganglioside GM1 on the circulation time of liposomes and on the target binding of immunoliposomes in vivo. *FEBS Lett* **1991,** 284, (2), 263-6.

76. Jokerst, J. V.; Lobovkina, T.; Zare, R. N.; Gambhir, S. S., Nanoparticle PEGylation for imaging and therapy. *Nanomedicine (Lond)* **2011,** 6, (4), 715-28.

77. Fisher, K. D.; Seymour, L. W., HPMA copolymers for masking and retargeting of therapeutic viruses. *Advanced drug delivery reviews* **2010,** 62, (2), 240-5.

78. Liu, J.; Bauer, H.; Callahan, J.; Kopeckova, P.; Pan, H.; Kopecek, J., Endocytic uptake of a large array of HPMA copolymers: Elucidation into the dependence on the physicochemical characteristics. *Journal of controlled release : official journal of the Controlled Release Society* **2010,** 143, (1), 71-9.

79. Andorko, J. I.; Pineault, K. G.; Jewell, C. M., Impact of molecular weight on the intrinsic immunogenic activity of poly(beta amino esters). *J Biomed Mater Res A* **2017,** 105, (4), 1219-1229.

80. Wegmann, F.; Gartlan, K. H.; Harandi, A. M.; Brinckmann, S. A.; Coccia, M.; Hillson, W. R.; Kok, W. L.; Cole, S.; Ho, L. P.; Lambe, T.; Puthia, M.; Svanborg, C.; Scherer, E. M.; Krashias, G.; Williams, A.; Blattman, J. N.; Greenberg, P. D.; Flavell, R. A.; Moghaddam, A. E.; Sheppard, N. C.; Sattentau, Q. J., Polyethyleneimine is a potent mucosal adjuvant for viral glycoprotein antigens. *Nat Biotechnol* **2012,** 30, (9), 883-8.

81. Luo, M.; Wang, H.; Wang, Z.; Cai, H.; Lu, Z.; Li, Y.; Du, M.; Huang, G.; Wang, C.; Chen, X.; Porembka, M. R.; Lea, J.; Frankel, A. E.; Fu, Y. X.; Chen, Z. J.; Gao, J., A STING-activating nanovaccine for cancer immunotherapy. *Nat Nanotechnol* **2017,** 12, (7), 648-654.

82. Wille-Reece, U.; Wu, C. Y.; Flynn, B. J.; Kedl, R. M.; Seder, R. A., Immunization with HIV-1 Gag protein conjugated to a TLR7/8 agonist results in the generation of HIV-1 Gag-specific Th1 and CD8+ T cell responses. *J Immunol* **2005,** 174, (12), 7676-83.

83. Kranz, L. M.; Diken, M.; Haas, H.; Kreiter, S.; Loquai, C.; Reuter, K. C.; Meng, M.; Fritz, D.; Vascotto, F.; Hefesha, H.; Grunwitz, C.; Vormehr, M.; Husemann, Y.; Selmi, A.; Kuhn, A. N.; Buck, J.; Derhovanessian, E.; Rae, R.; Attig, S.; Diekmann, J.; Jabulowsky, R. A.; Heesch, S.; Hassel, J.; Langguth, P.; Grabbe, S.; Huber, C.; Tureci, O.; Sahin, U., Systemic RNA delivery to dendritic cells exploits antiviral defence for cancer immunotherapy. *Nature* **2016,** 534, (7607), 396-401.

84. Reddy, S. T.; van der Vlies, A. J.; Simeoni, E.; Angeli, V.; Randolph, G. J.; O'Neil, C. P.; Lee, L. K.; Swartz, M. A.; Hubbell, J. A., Exploiting lymphatic transport and complement activation in nanoparticle vaccines. *Nat Biotechnol* **2007,** 25, (10), 1159-64.

85. Haas, T.; Schmitz, F.; Heit, A.; Wagner, H., Sequence independent interferon-alpha induction by multimerized phosphodiester DNA depends on spatial regulation of Toll-like receptor-9 activation in plasmacytoid dendritic cells. *Immunology* **2009,** 126, (2), 290-8.

86. Honda, K.; Ohba, Y.; Yanai, H.; Negishi, H.; Mizutani, T.; Takaoka, A.; Taya, C.; Taniguchi, T., Spatiotemporal regulation of MyD88-IRF-7 signalling for robust type-I interferon induction. *Nature* **2005,** 434, (7036), 1035-40.

87. Qu, C.; Nguyen, V. A.; Merad, M.; Randolph, G. J., MHC class I/peptide transfer between dendritic cells overcomes poor cross-presentation by monocyte-derived APCs that engulf dying cells. *J Immunol* **2009,** 182, (6), 3650-9.

88. Kim, T. S.; Braciale, T. J., Respiratory dendritic cell subsets differ in their capacity to support the induction of virus-specific cytotoxic CD8+ T cell responses. *PLoS One* **2009,** 4, (1), e4204.

TABLE OF CONENTS GRAPHIC